Copy No. 124

RM No. A7J23

CONFIDENTIAL

NACA

RESEARCH MEMORANDUM

HIGH-SPEED AERODYNAMIC CHARACTERISTICS OF FOUR THIN NACA 63-SERIES AIRFOILS

By Richard J. Ilk

Ames Aeronautical Laboratory
Moffett Field, Calif.

NATIONAL ADVISORY COMMITTEE FOR AERONAUTICS

WASHINGTON

December 31, 1947

CONFIDENTIAL

NACA RM No. A7J23

CONFIDENTIAL

NATIONAL ADVISORY COMMITTEE FOR AERONAUTICS

RESEARCH MEMORANDUM

HIGH-SPEED AERODYNAMIC CHARACTERISTICS OF FOUR THIN NACA 63-SERIES AIRFOILS

By Richard J. Ilk

SUMMARY

High-speed wind-tunnel tests have been made of four thin NACA 63-series airfoil sections having a design lift coefficient of 0.2 with the uniform-load type of mean camber line to determine the effectiveness of forward movement of the minimum-pressure position in improving the high-speed lift characteristics of low-drag airfoils. Section aerodynamic characteristics at constant angles of attack from -6° to 12° are presented for Mach numbers from 0.3 to 0.875. The data obtained are compared to similar data for corresponding NACA 64-series airfoils.

For NACA 6-series airfoils less than 12-percent chord thick, movement of minimum pressure from the 40-percent- to the 30-percent-chord location results in somewhat poorer high-speed aerodynamic characteristics with regard to force-divergence Mach numbers and lift-curve slope, although the differences are small. The supercritical-speed lift characteristics of the NACA 63-212 airfoil are slightly better than those of the NACA 64-212 section. Thin NACA 6-series airfoils with minimum-pressure positions ranging from 30 percent to 60 percent of the airfoil chord appear to exhibit optimum high-speed aerodynamic characteristics with the minimum-pressure position at 40 percent of the airfoil chord from the leading edge. For even the thinnest airfoil sections, the range of lift coefficients over which high force-divergence Mach numbers are maintained appears to be sufficiently broad to satisfy normal flight requirements.

INTRODUCTION

High-speed wind-tunnel tests (reference 1) of a group of thin NACA 64-, 65-, and 66-series airfoils having an ideal lift coefficient of 0.2 with the uniform-load type of mean camber line have indicated increasingly better over-all high-speed aerodynamic characteristics with forward movement of minimum pressure from the 60- to

the 40-percent-chord location. To investigate the possibility of additional gains in supercritical lift characteristics with still further forward movement of minimum pressure on NACA 6-series airfoils, tests of four NACA 63-series airfoils having thickness-chord ratios corresponding to those of the airfoils of reference 1 were undertaken in the Ames 1- by 3½-foot high-speed wind tunnel. From the results of this investigation it was hoped that an optimum minimum-pressure position could be determined for NACA 6-series airfoils having a design lift coefficient of 0.2 to be employed on high-speed aircraft.

APPARATUS AND TESTS

The present investigation was conducted in the Ames 1- by 3½-foot high-speed wind tunnel. This tunnel is a two-dimensional-flow, low-turbulence, closed-throat type and is powered by two 1000-horsepower motors.

Four 6-inch-chord models, representing the NACA 63-206, 63-208, 63-210, and 63-212 airfoil sections having uniform-load type ($a = 1.0$) mean camber lines, were constructed of duralumin for the tests. The airfoil ordinates are presented in table I and profile sketches of the sections appear in figure 1.

Each airfoil model was mounted so as to completely span the 1-foot dimension of the tunnel test section, as illustrated in figure 2. Sponge-rubber gaskets were compressed between the tunnel walls and the ends of the models to prevent end leakage, thereby preserving two-dimensional flow and assuring the measurement of true section characteristics.

Simultaneous measurements of section lift, drag, and pitching moment were made at angles of attack ranging from -6° to 12° by increments of 2°. Each model was tested at angles of attack sufficiently high to determine the lift stall at all but the highest Mach numbers. The free-stream Mach number was varied from 0.3 to 0.375 and the corresponding Reynolds number variation (fig. 3) was from 1×10^6 to nearly 2×10^6 for the 6-inch-chord models.

Lift forces and pitching moments were determined from tunnel-wall-reaction measurements by a method similar to that for measuring lift forces described in the appendix to reference 2. Drag forces were measured by means of the wake-survey method in which a movable 9-inch-wide rake of 35 total-head tubes was employed. At the choking Mach number, the airfoil wake extended from the floor to the ceiling

of the test section, thus making it impossible to accurately evaluate the drag. The method described in reference 3 was used for computing the drag coefficients.

It is believed that angle-of-attack values are accurate to $\pm 0.1^\circ$ and relative angles for any one airfoil are valid to within $\pm 0.05^\circ$. The extensive Mach number range over which the Ames 1- by $3\frac{1}{2}$-foot high-speed wind tunnel is operated necessitates equipment capable of measuring a large range of forces. The low-speed results, particularly the pitching-moment values, may be unduly affected by errors in tares and zero readings which are of negligible magnitude at higher speeds.

RESULTS AND DISCUSSION

Tunnel-Wall Effects

With the exception of characteristics measured at the choked-flow condition, all data of the present tests have been corrected for wind-tunnel-wall interference by the methods of reference 4. It has been demonstrated in this reference that data obtained under choked-flow conditions cannot be corrected to free-air characteristics because no equivalent free-air flow exists. Accordingly, broken lines have been used to indicate that some uncertainty exists regarding the validity of data obtained at Mach numbers in the vicinity of the wind-tunnel choking Mach number.

Lift Coefficient

Lift coefficients at constant angles of attack for each of the four thin NACA 63-series airfoils are plotted as a function of free-stream Mach number in figures 4 to 7. Corresponding cross plots (figs. 8 to 11) at constant Mach number present the variation of section lift coefficient with angle of attack. The lift characteristics of NACA 63-series airfoils appear to be qualitatively similar to corresponding data for NACA 64-, 65-, and 66-series airfoils as presented in reference 1.

Lift-divergence Mach numbers for each airfoil are plotted in figure 12 as a function of section lift coefficient. The Mach number for lift-divergence is defined as the lowest Mach number corresponding to an inflection point on the curve of section lift coefficient versus Mach number at constant angle of attack. A comparison of the lift-divergence data of figure 12 with similar data of reference 1 for

NACA 64-series airfoils shows that, for approximately equal ranges of useful lift coefficient, the NACA 63-212 airfoil has a slightly higher value of lift-divergence Mach number than the NACA 64-212 airfoil. However, the lift-divergence Mach numbers for NACA 63-series airfoils less than 12-percent chord thick are lower than those for NACA 64-series airfoils of comparable thickness-chord ratios. It appears, however, that the range of lift coefficients over which the NACA 63-series airfoils exhibit high lift-divergence Mach numbers remains sufficiently broad to satisfy normal high-speed flight requirements. The effect of thickness-chord ratio on the lift-divergence Mach number, shown by figure 13, indicates that a decrease in airfoil thickness-chord ratio increases the lift-divergence Mach number, but thickness variation appears to have no consistent effect on the extent of the useful lift coefficient range.

The variation of lift-curve slope with Mach number, as affected by thickness-chord ratio and minimum-pressure position, is presented in figures 14 and 15. The curves of figure 14 show no consistent variation of lift-curve slope with changes in thickness-chord ratio except at the highest speeds where the lift-curve slope appears to increase progressively as the airfoil thickness-chord ratio decreases. The Mach number at which the lift-curve slope attains a maximum value for a given airfoil decreases with increasing thickness-chord ratio. The lift-curve slope reaches the maximum value at a higher Mach number for the NACA 63-212 than for the NACA 64-212 airfoil. (See fig. 15.) For all the airfoils less than 12-percent chord thick, however, forward movement of the minimum-pressure position from the 40-percent- to the 30-percent-chord station causes an earlier decrease in the lift-curve slope.

An analysis of maximum-lift-coefficient data (reference 5) obtained from full-scale flight tests and from several high-speed wind-tunnel tests has shown that the effect of Reynolds number on the maximum lift coefficient decreases with increasing Mach number and vanishes at a Mach number of approximately 0.55. Thus, it can be assumed that the maximum lift coefficients obtained at Mach numbers of 0.6 and above in the present test are reliable at full-scale Reynolds numbers.

In figure 16, the variation of maximum lift coefficient with Mach number is shown for the NACA 63-series airfoils tested. The curves of this figure indicate that at Mach numbers greater than 0.7 the maximum lift coefficient increases with progressively decreasing thickness-chord ratios. The curves of figure 17, which present the effect of minimum-pressure position on the maximum lift

coefficient, show that the values of maximum lift coefficient for the NACA 63-212 airfoil exceed those of the NACA 64-212 airfoil above a Mach number of 0.675. NACA 6-series airfoils less than 12-percent chord thick exhibit lower values of maximum lift coefficient with the minimum pressure at the 30-percent- rather than the 40-percent-chord position.

The variation in angle of zero lift with Mach number is shown in figure 18 for NACA 63-series airfoils of various thickness-chord ratios and in figure 19 for comparable NACA 63- and 64-series airfoils. The angle of zero lift appears to have no consistent variation with thickness-chord ratio (fig. 18) but forward movement of the minimum pressure, from the 40-percent- to the 30-percent-chord position, tends to shift the values closer to 0° as shown by figure 19. With an increase in Mach number, the angle of zero lift remains fairly constant until the critical Mach number of the airfoil has been exceeded, after which it increases in the direction of 0°. This increase in the zero-lift angle has an adverse effect on level-flight trim conditions and greatly affects high-speed stability. Movement of minimum pressure from the 40-percent- to the 30-percent-chord position results in no significant change in the variation of angle of zero lift with Mach number. (See fig. 19.)

Drag Coefficient

Curves of section drag coefficient versus Mach number are presented in figures 20 to 23 for the four NACA 63-series airfoils at constant angles of attack. Corresponding cross plots of section drag coefficient as a function of lift coefficient for constant Mach numbers are shown in figures 24 to 27. From the curves of figures 20 to 23, it can be seen that, at small angles of attack, the value of the drag coefficient remains nearly constant until the critical speed of the airfoil has been exceeded. At higher angles of attack the drag coefficient experiences a decrease immediately preceding the final abrupt drag rise. This same effect was observed in the tests reported in reference 1 and it appears to be characteristic of NACA 6-series airfoils at the Reynolds numbers of the present tests.

The Mach number of drag divergence for a given airfoil angle of attack is arbitrarily defined as the Mach number at which the slopes of the drag curves of figures 20 to 23 are equal to 0.10. The drag-divergence Mach numbers determined by this criterion are in good agreement with those obtained by the method of reference 1. In figure 28, the drag-divergence Mach numbers for each airfoil

are plotted as a function of section lift coefficient. From a comparison of the curves of figure 28 with similar data of reference 1, it can be seen that both the Mach number for drag divergence and the extent of the lift-coefficient range over which high drag-divergence Mach numbers are exhibited decrease as the minimum pressure advances from the 40-percent- to the 30-percent-chord location. That a decrease in airfoil thickness-chord ratio delays the onset of the abrupt drag rise to higher Mach numbers is indicated by the data of figure 28 which presents the effect of thickness-chord ratio on the Mach numbers for drag divergence.

The variation of the section drag coefficient with Mach number at the design lift coefficient for the NACA 63-series airfoils is compared to corresponding data for NACA 64-series airfoils in figure 29. This comparison indicates that the high-speed drag characteristics of the NACA 64-series airfoils are slightly better than those of the NACA 63-series airfoils.

Moment Coefficient

Quarter-chord pitching-moment coefficients at constant angles of attack are presented as a function of Mach number in figures 30 to 33 for each of the NACA 63-series airfoils. The pitching-moment data are cross plotted as a function of section lift coefficient in figures 34 to 37. For airfoils cambered with the uniform-load type of mean line, the experimental moment coefficients are usually less than would be predicted from thin-airfoil theory. (See reference 2.) In figures 34 to 37, the low-speed experimental values of quarter-chord moment coefficient at the design lift coefficient agree fairly well with the theoretical coefficient of -0.05 (reference 2) for the $a = 1.0$ mean line. The difference between the theoretical and the low-speed experimental quarter-chord moment coefficient, particularly for the NACA 64-208 airfoil (fig. 39), is probably due to a slightly warped camber line resulting from construction errors.

The effects of airfoil thickness and position of minimum pressure on the variation of moment coefficient with Mach number at the design lift coefficient are shown in figures 38 and 39. Neither variation in the thickness-chord ratio (fig. 38) nor forward movement of the minimum pressure (fig. 39) appears to cause a consistent variation in the pitching-moment coefficient.

CONCLUSIONS

From high-speed wind-tunnel tests of four NACA 63-series airfoils, and from previous wind-tunnel tests of corresponding NACA 6-series profiles, several conclusions are drawn:

1. NACA 63-series airfoil sections of thickness-chord ratios less than 0.12 exhibit somewhat poorer aerodynamic characteristics for high-speed applications with regard to force-divergence Mach numbers and lift-curve slope than do corresponding NACA 64-series airfoil sections, the differences being small, however.

2. The NACA 63-212 airfoil section is slightly more suitable for high Mach number applications than the NACA 64-212 from the standpoint of supercritical-speed lift characteristics.

3. For NACA 6-series airfoils with minimum pressure positions ranging from 30 percent to 60 percent of the airfoil chord, optimum high-speed aerodynamic characteristics would appear to be derived from those airfoils having the location of minimum pressure at 40 percent of the airfoil chord from the leading edge.

Ames Aeronautical Laboratory,
National Advisory Committee for Aeronautics,
Moffett Field, Calif.

REFERENCES

1. Van Dyke, Milton D., and Wibbert, Gordon A.: High-Speed Aerodynamic Characteristics of 12 Thin NACA 6-Series Airfoils. NACA CMR No. A5F27, 1945.

2. Abbott, Ira H., von Doenhoff, Albert E., and Stivers, Louis S., Jr.: Summary of Airfoil Data. NACA ACR No. L5C05, 1945.

3. Heaslet, Max. A.: Theoretical Investigation of Methods for Computing Drag From Wake Surveys at High Subsonic Speeds. NACA ARR No. 5C21, 1945.

4. Allen, H. Julian, and Vincenti, Walter G.: Wall Interference in a Two-Dimensional-Flow Wind Tunnel with Consideration of the Effect of Compressibility. NACA ARR No. 4K03, 1944.

5. Spreiter, John R., and Steffen, Paul J.: Effect of Mach and Reynolds Numbers on Maximum Lift Coefficient. NACA TN No. 1044, 1946.

TABLE I.- ORDINATES OF THE NACA 63-SERIES AIRFOILS TESTED. NACA 63-206.

[Stations and ordinates given in percent of airfoil chord]

Upper surface		Lower surface	
Station	Ordinate	Station	Ordinate
0	0	0	0
.458	.551	.542	- .451
.703	.677	.797	- .537
1.197	.876	1.303	- .662
2.438	1.241	2.562	- .869
4.932	1.776	5.068	-1.144
7.429	2.189	7.571	-1.341
9.930	2.526	10.070	-1.492
14.934	3.058	15.066	-1.712
19.941	3.451	20.059	-1.859
24.950	3.736	25.050	-1.946
29.960	3.926	30.040	-1.982
34.970	4.030	35.030	-1.970
39.981	4.042	40.019	-1.900
44.991	3.972	45.009	-1.782
50.000	3.826	50.000	-1.620
55.008	3.612	54.992	-1.422
60.015	3.338	59.985	-1.196
65.020	3.012	64.980	- .952
70.023	2.642	69.977	- .698
75.023	2.237	74.977	- .447
80.022	1.804	79.978	- .212
85.019	1.356	84.981	- .010
90.013	.900	89.987	.134
95.006	.454	94.993	.178
100.000	0	100.000	0

L. E. radius: 0.297
Slope of radius through L.E.: 0.0842

TABLE I.- Continued. NACA 63-208.

[Stations and ordinates given in percent of airfoil chord]

Upper surface		Lower surface	
Station	Ordinate	Station	Ordinate
0	0	0	0
.444	.715	.556	- .615
.687	.876	.813	- .736
1.179	1.131	1.321	- .917
2.418	1.592	2.582	-1.220
4.909	2.266	5.091	-1.634
7.406	2.780	7.594	-1.932
9.906	3.201	10.094	-2.167
14.912	3.861	15.088	-2.515
19.922	4.345	20.078	-2.753
24.934	4.690	25.066	-2.900
29.947	4.918	30.053	-2.974
34.961	5.030	35.039	-2.970
39.974	5.027	40.026	-2.885
44.988	4.919	45.012	-2.729
50.000	4.717	50.000	-2.511
55.011	4.429	54.989	-2.239
60.019	4.069	59.981	-1.927
65.026	3.645	64.974	-1.585
70.030	3.170	69.970	-1.226
75.031	2.657	74.969	- .867
80.029	2.115	79.971	- .523
85.025	1.563	84.975	- .217
90.017	1.013	89.983	.021
95.008	.494	94.992	.138
100.000	0	100.000	0

L. E. radius: 0.503
Slope of radius through L.E.: 0.0842

TABLE I.- Continued. NACA 63-210.

[Stations and ordinates given in percent of airfoil chord]

Upper surface		Lower surface	
Station	Ordinate	Station	Ordinate
0	0	0	0
.430	.876	.570	- .776
.669	1.107	.831	- .967
1.162	1.379	1.338	-1.165
2.398	1.939	2.602	-1.567
4.886	2.753	5.114	-2.121
7.382	3.372	7.618	-2.524
9.882	3.877	10.118	-2.843
14.890	4.666	15.110	-3.320
19.902	5.240	20.098	-3.648
24.917	5.647	25.083	-3.857
29.933	5.910	30.067	-3.966
34.951	6.030	35.049	-3.970
39.968	6.009	40.032	-3.867
44.985	5.861	45.015	-3.671
50.000	5.599	50.000	-3.393
55.013	5.235	54.987	-3.045
60.024	4.786	59.976	-2.644
65.032	4.264	64.968	-2.205
70.037	3.684	69.963	-1.740
75.038	3.061	74.962	-1.271
80.036	2.414	79.964	- .822
85.030	1.761	84.970	- .415
90.021	1.121	89.979	- .087
95.010	.530	94.990	.102
100.000	0	100.000	0

L. E. radius: 0.770
Slope of radius through L.E.: 0.0842

TABLE I.- Concluded. NACA 63-212.

[Stations and ordinates given in percent of airfoil chord]

Upper surface		Lower surface	
Station	Ordinate	Station	Ordinate
0	0	0	0
.417	1.032	.583	- .932
.657	1.260	.843	-1.120
1.145	1.622	1.355	-1.408
2.378	2.284	2.622	-1.912
4.863	3.238	5.137	-2.606
7.358	3.963	7.642	-3.115
9.859	4.554	10.141	-3.520
14.868	5.470	15.132	-4.124
19.882	6.137	20.118	-4.545
24.900	6.606	25.100	-4.816
29.920	6.902	30.080	-4.958
34.941	7.030	35.059	-4.970
39.962	6.991	40.038	-4.849
44.982	6.799	45.018	-4.609
50.000	6.473	50.000	-4.267
55.016	6.030	54.984	-3.840
60.029	5.491	59.971	-3.349
65.038	4.870	64.962	-2.810
70.043	4.182	69.957	-2.238
75.045	3.451	74.955	-1.661
80.042	2.698	79.958	-1.106
85.035	1.947	84.965	- .601
90.025	1.224	89.975	- .190
95.012	.566	94.988	.066
100.000	0	100.000	0

L. E. radius: 1.087
Slope of radius through L.E.: 0.0842

CONFIDENTIAL

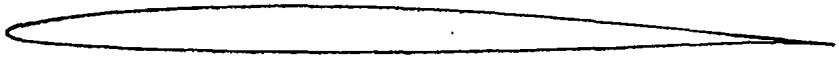

NACA 63-206

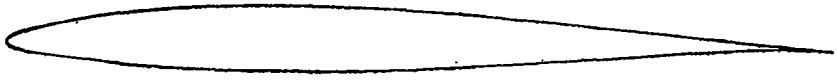

NACA 63-208

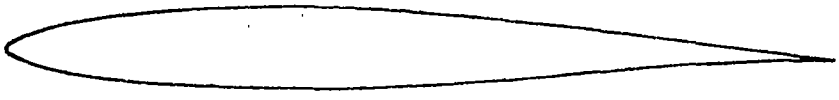

NACA 63-210

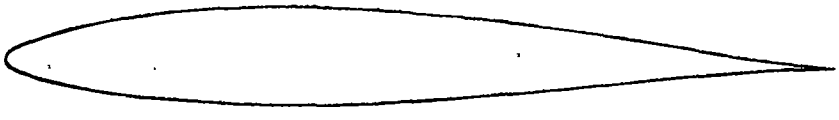

NACA 63-212

NATIONAL ADVISORY
COMMITTEE FOR AERONAUTICS

FIGURE 1.- NACA 63-SERIES AIRFOIL SECTIONS HAVING UNIFORM-LOAD TYPE ($a=1.0$) MEAN CAMBER LINE.

CONFIDENTIAL

Figure 2.– Airfoil model mounted in the test section of the Ames 1– by $3\frac{1}{2}$–foot high–speed wind tunnel.

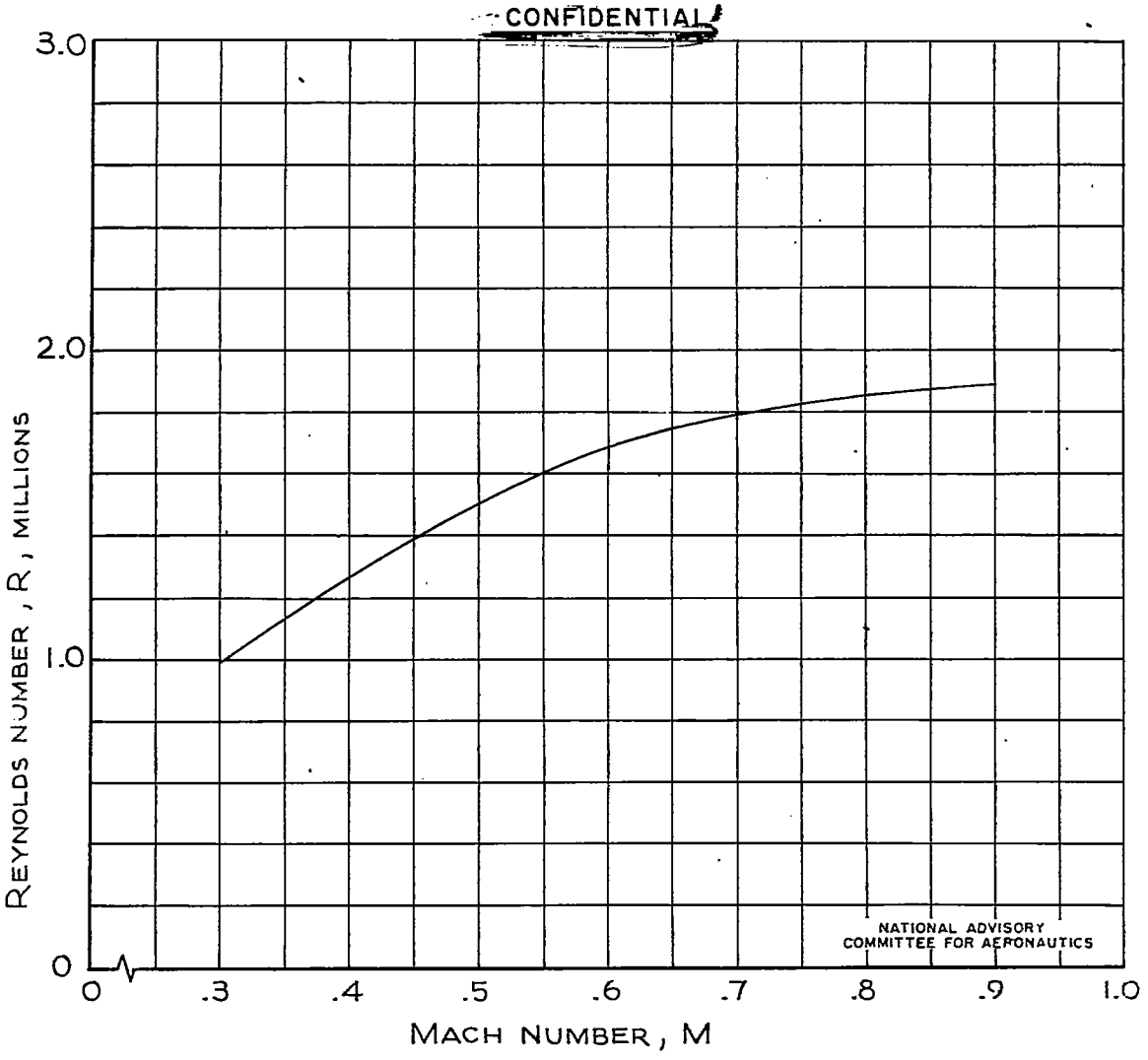

FIGURE 3.- THE VARIATION OF REYNOLDS NUMBER WITH MACH NUMBER FOR A 6-INCH-CHORD AIRFOIL IN THE AMES 1-BY $3\frac{1}{2}$-FOOT HIGH-SPEED WIND TUNNEL. CONFIDENTIAL

Fig. 4

CONFIDENTIAL

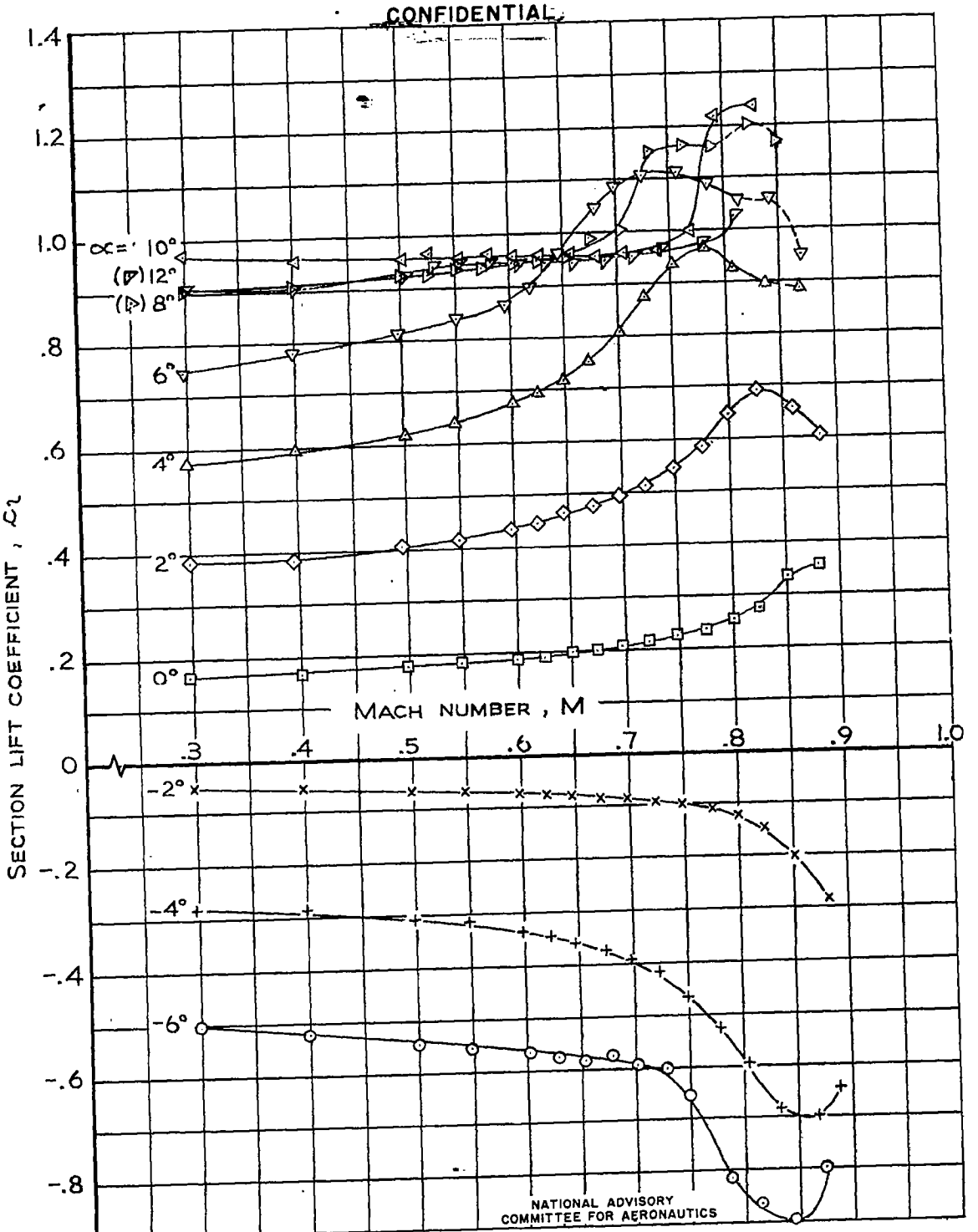

FIGURE 4.-THE VARIATION OF SECTION LIFT COEFFICIENT WITH MACH NUMBER FOR THE NACA 63-206 AIRFOIL.

CONFIDENTIAL

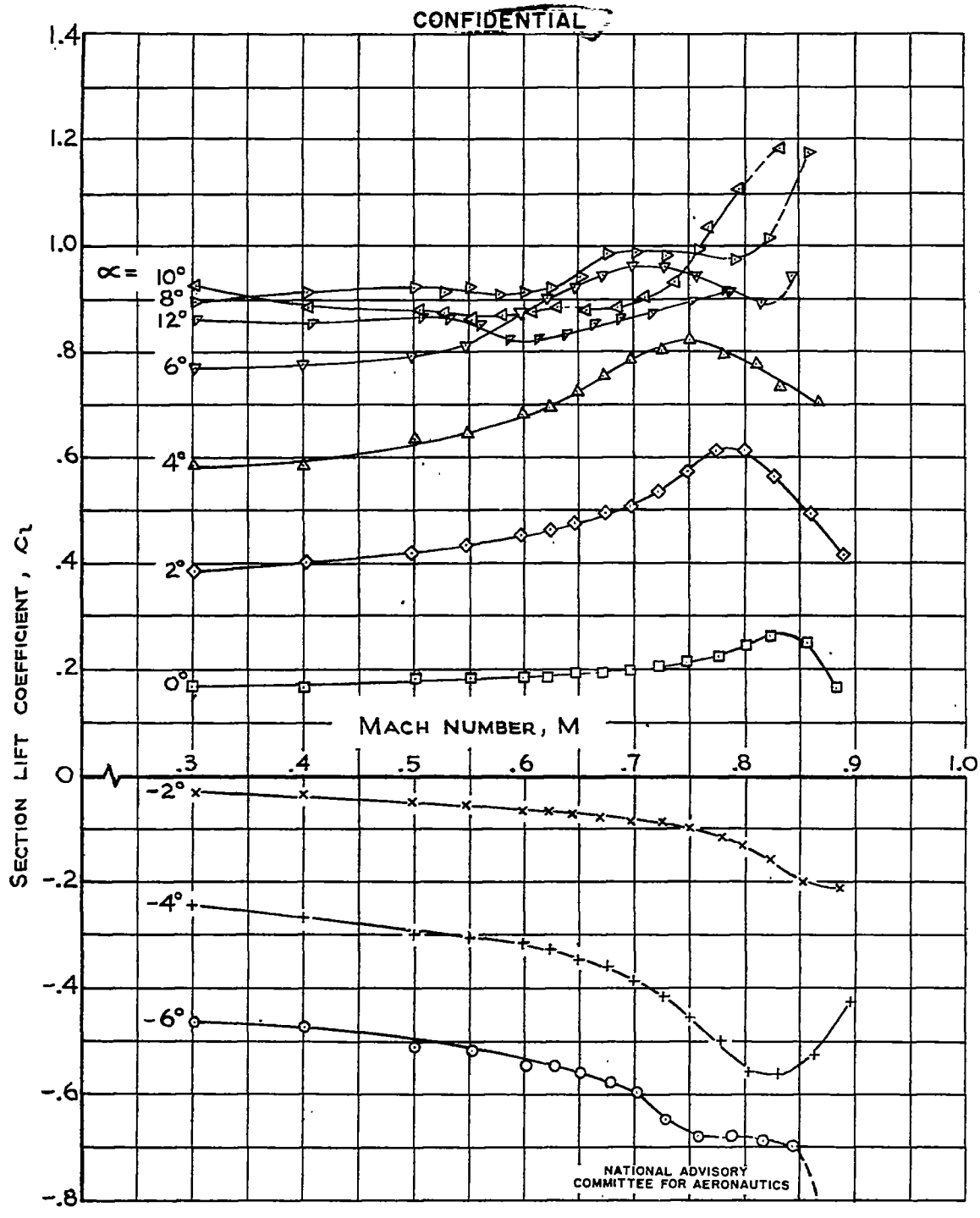

FIGURE 5.—THE VARIATION OF SECTION LIFT COEFFICIENT WITH MACH NUMBER FOR THE NACA 63-208 AIRFOIL.

CONFIDENTIAL

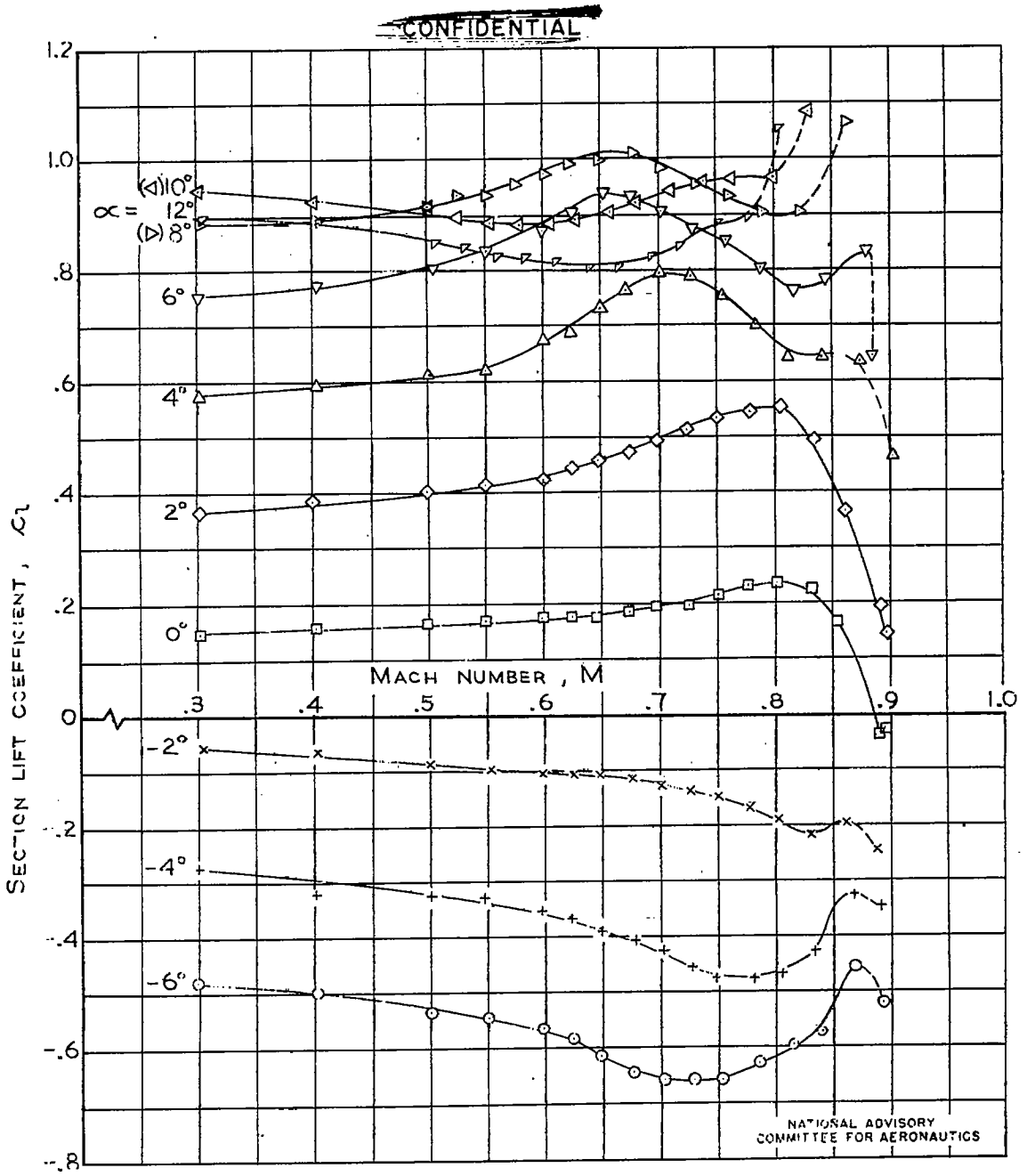

FIGURE 6.-THE VARIATION OF SECTION LIFT COEFFICIENT WITH MACH NUMBER FOR THE NACA 63-210 AIRFOIL.

CONFIDENTIAL

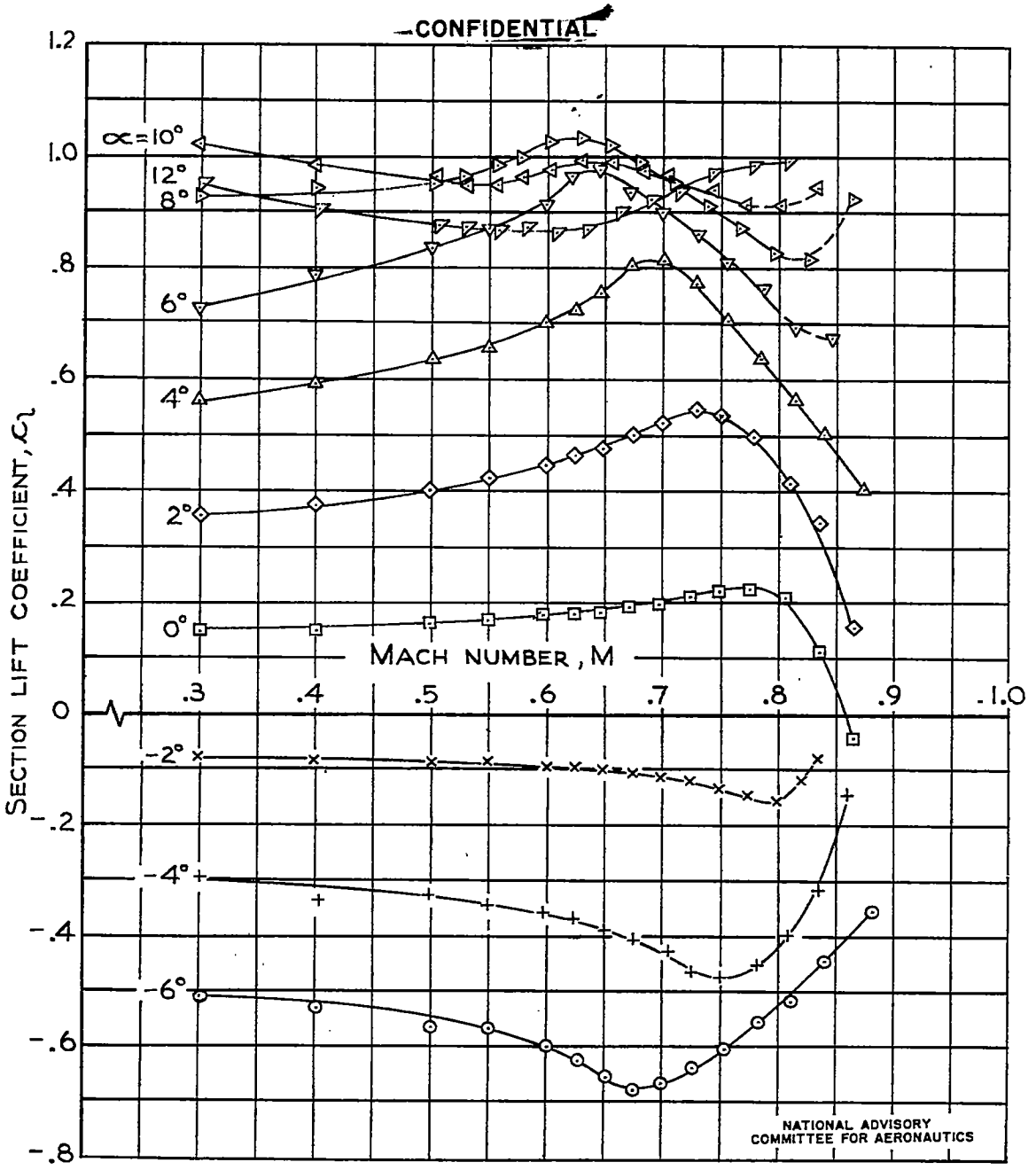

FIGURE 7.-THE VARIATION OF SECTION LIFT COEFFICIENT WITH MACH NUMBER FOR THE NACA 63-212 AIRFOIL.

CONFIDENTIAL

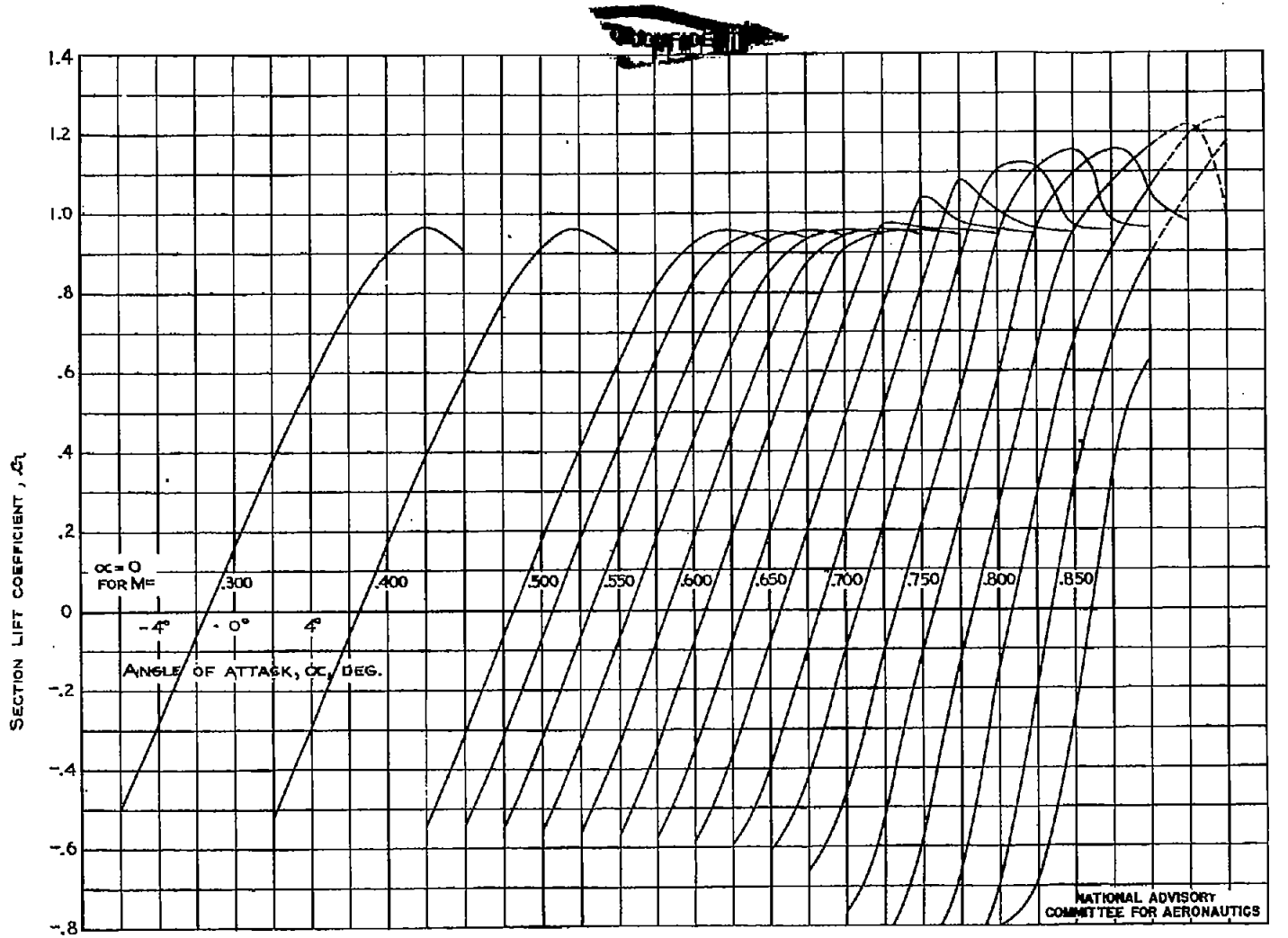

FIGURE 8.—THE VARIATION OF SECTION LIFT COEFFICIENT WITH ANGLE OF ATTACK FOR THE NACA 63-206 AIRFOIL.

CONFIDENTIAL

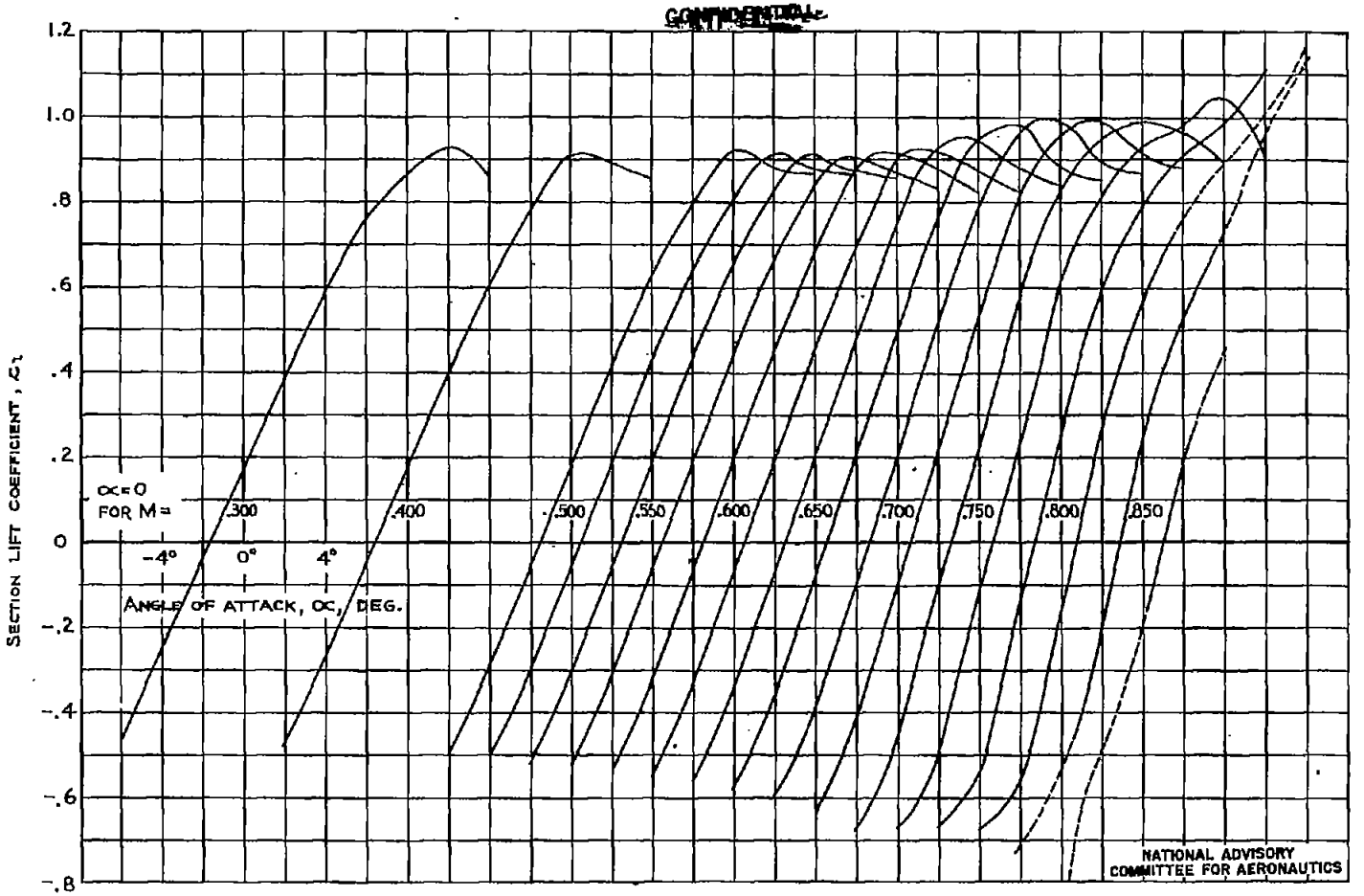

FIGURE 9.- THE VARIATION OF SECTION LIFT COEFFICIENT WITH ANGLE OF ATTACK FOR THE NACA 63-208 AIRFOIL.

CONFIDENTIAL

Fig. 9

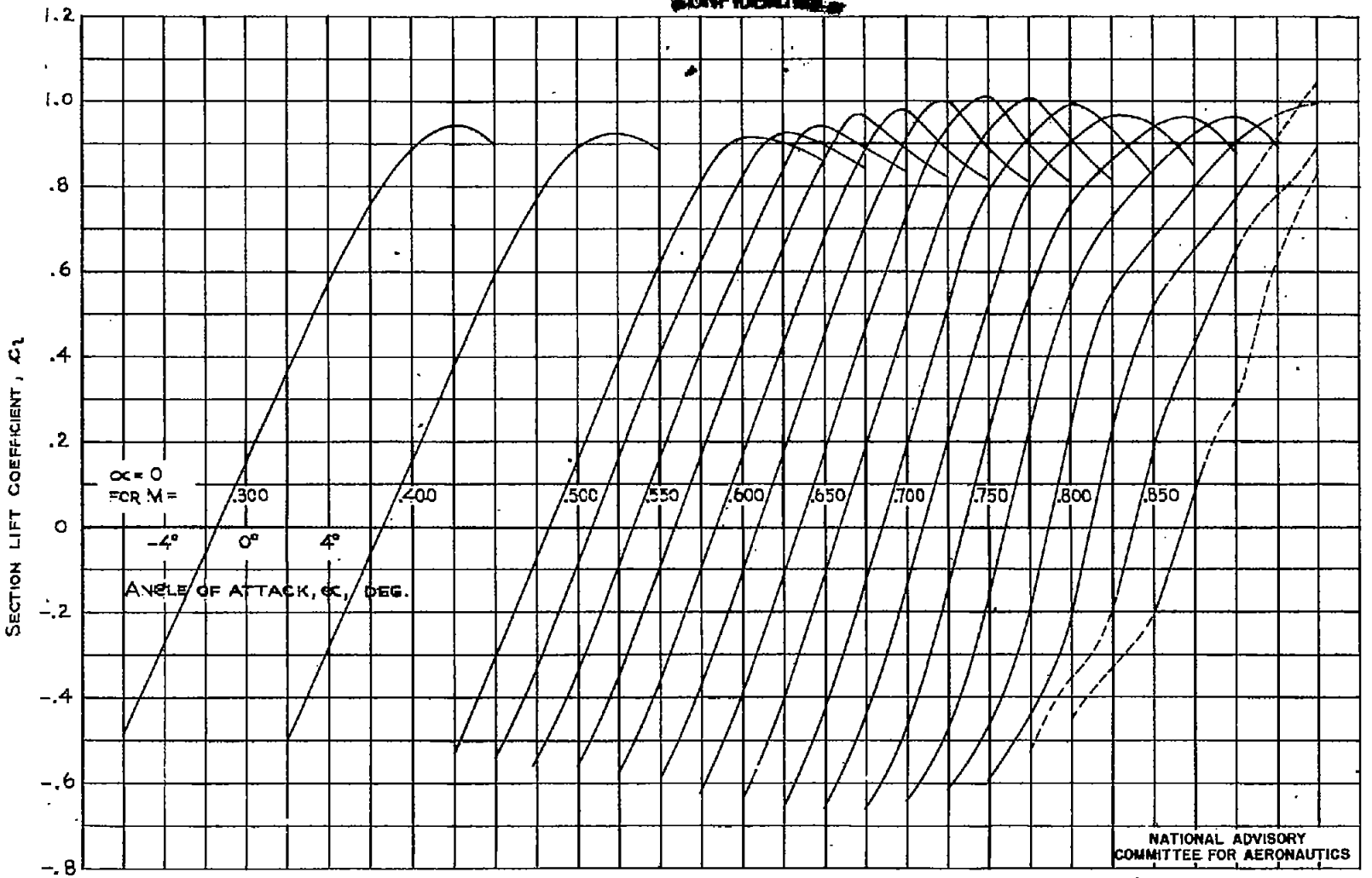

FIGURE 10.- THE VARIATION OF SECTION LIFT COEFFICIENT WITH ANGLE OF ATTACK FOR THE NACA 63-210 AIRFOIL.

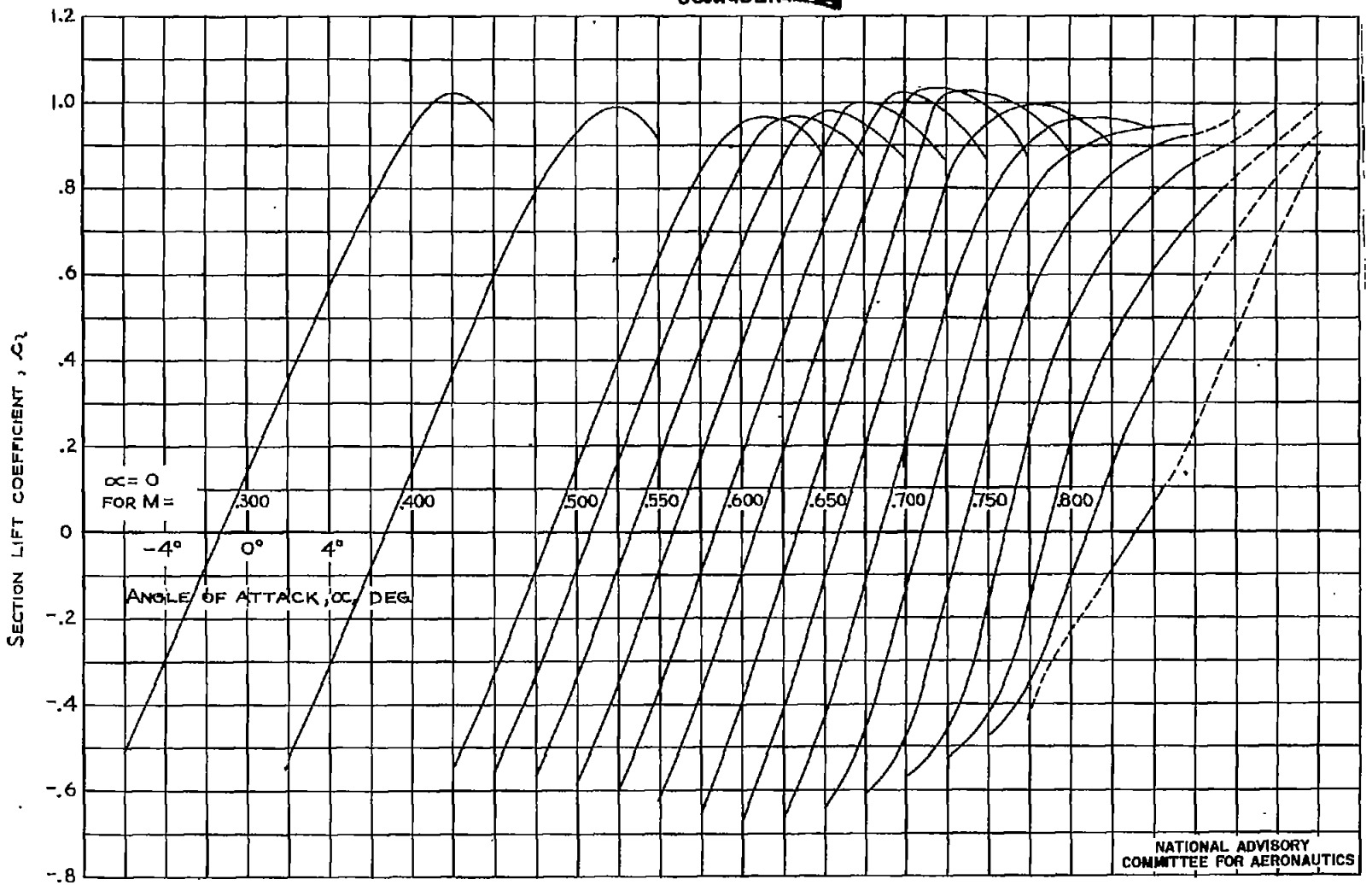

FIGURE 11.- THE VARIATION OF SECTION LIFT COEFFICIENT WITH ANGLE OF ATTACK FOR THE NACA 63-212 AIRFOIL.

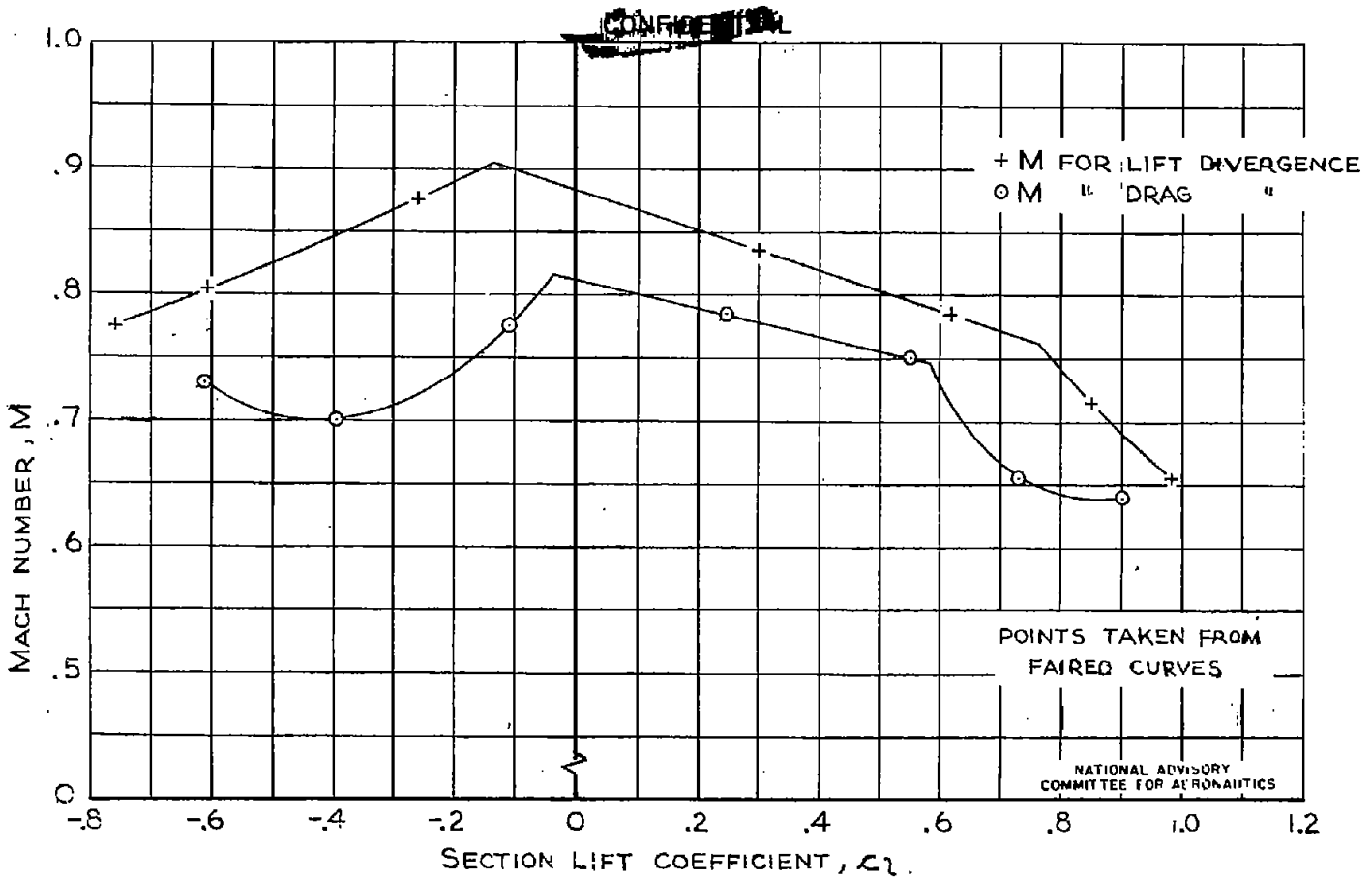

(a) NACA 63-206 AIRFOIL

FIGURE 12.- THE VARIATION OF LIFT- AND DRAG-DIVERGENCE MACH NUMBERS WITH SECTION LIFT COEFFICIENT FOR NACA 63-SERIES AIRFOILS

CONFIDENTIAL

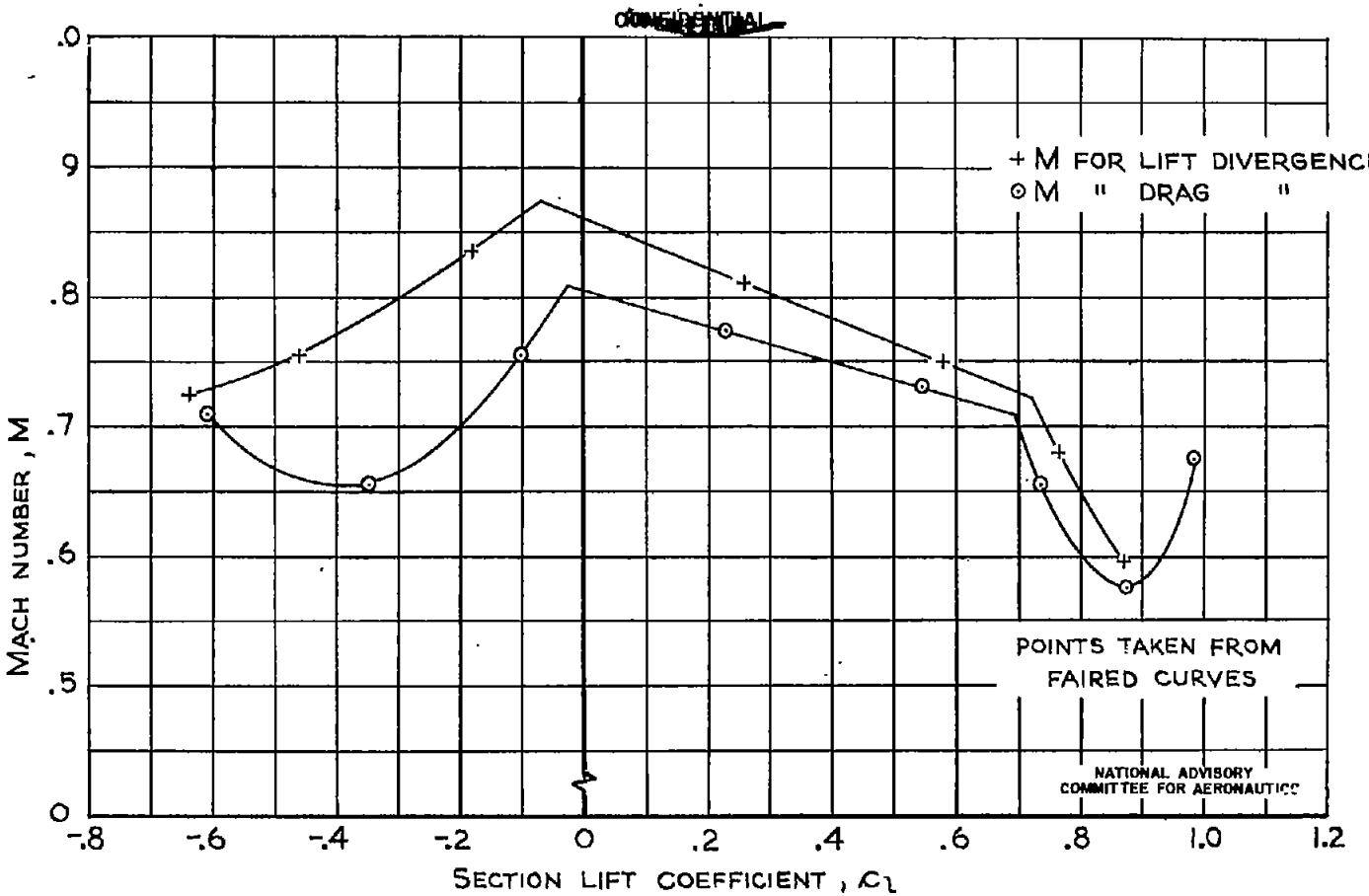

(b) NACA 63-208 AIRFOIL

FIGURE 12 - CONTINUED.

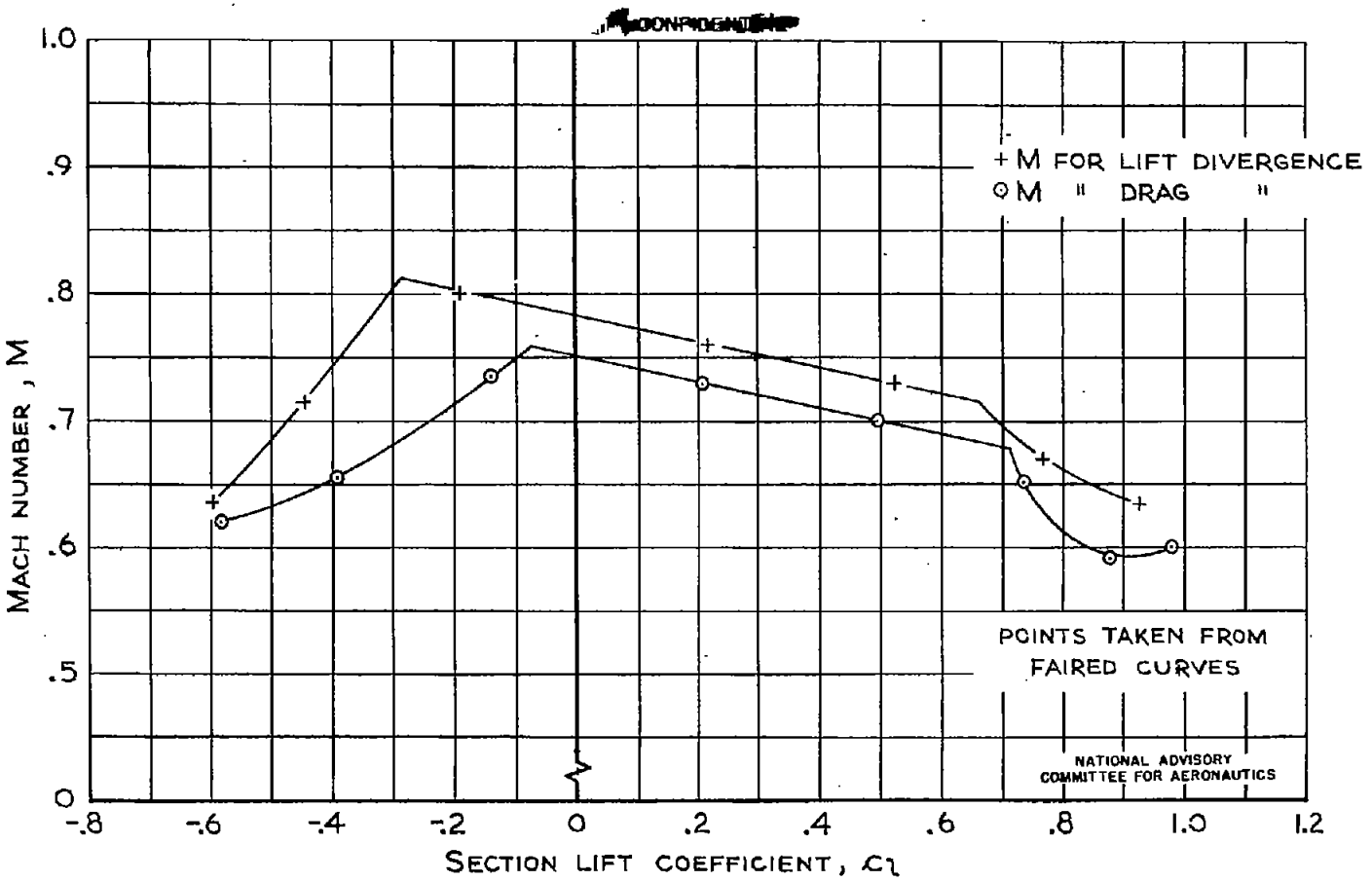

(c) NACA 63-210 AIRFOIL

FIGURE 12.- CONTINUED.

CONFIDENTIAL

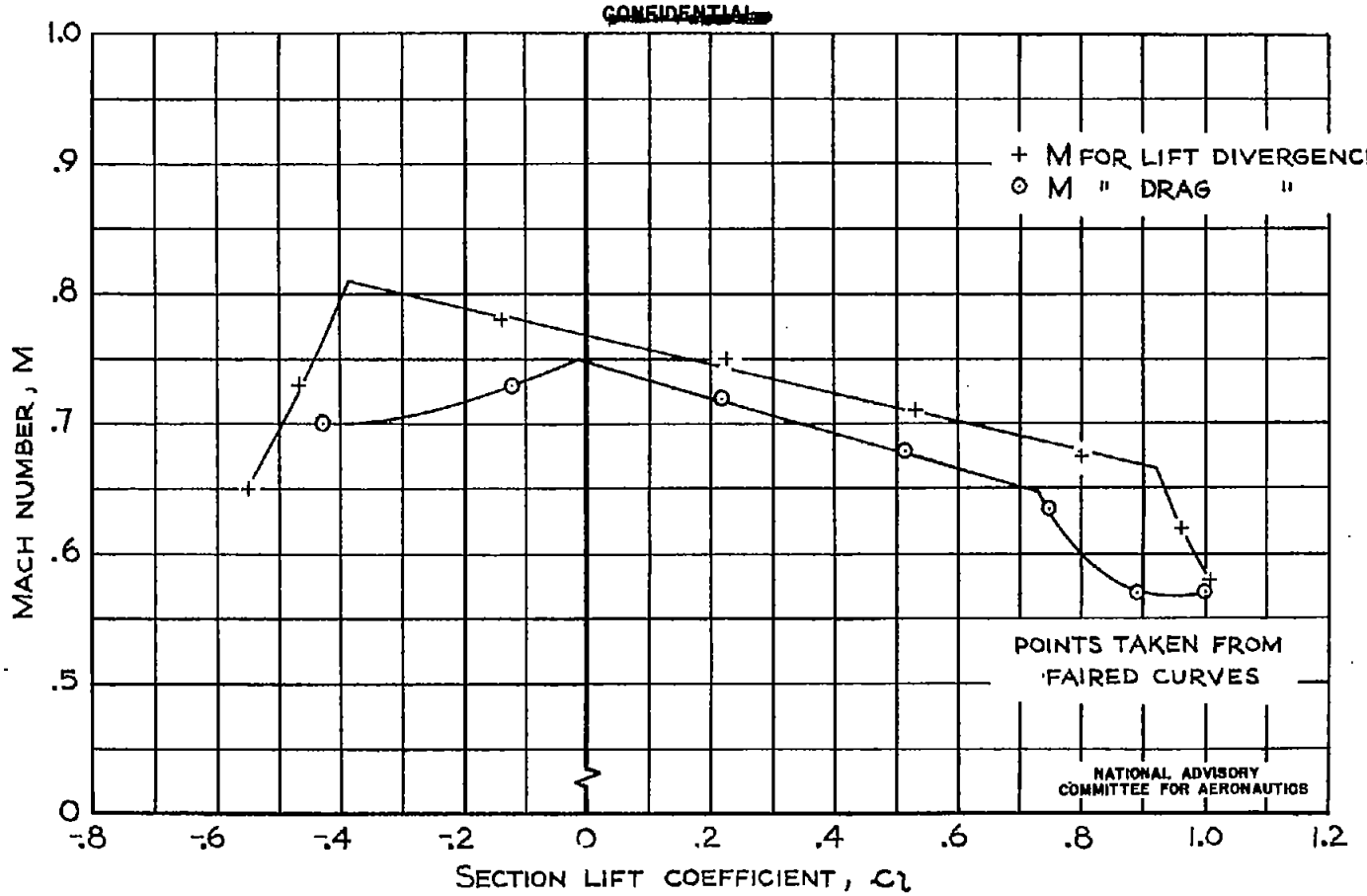

(d) NACA 63-212 AIRFOIL

FIGURE 12.-CONCLUDED.

CONFIDENTIAL

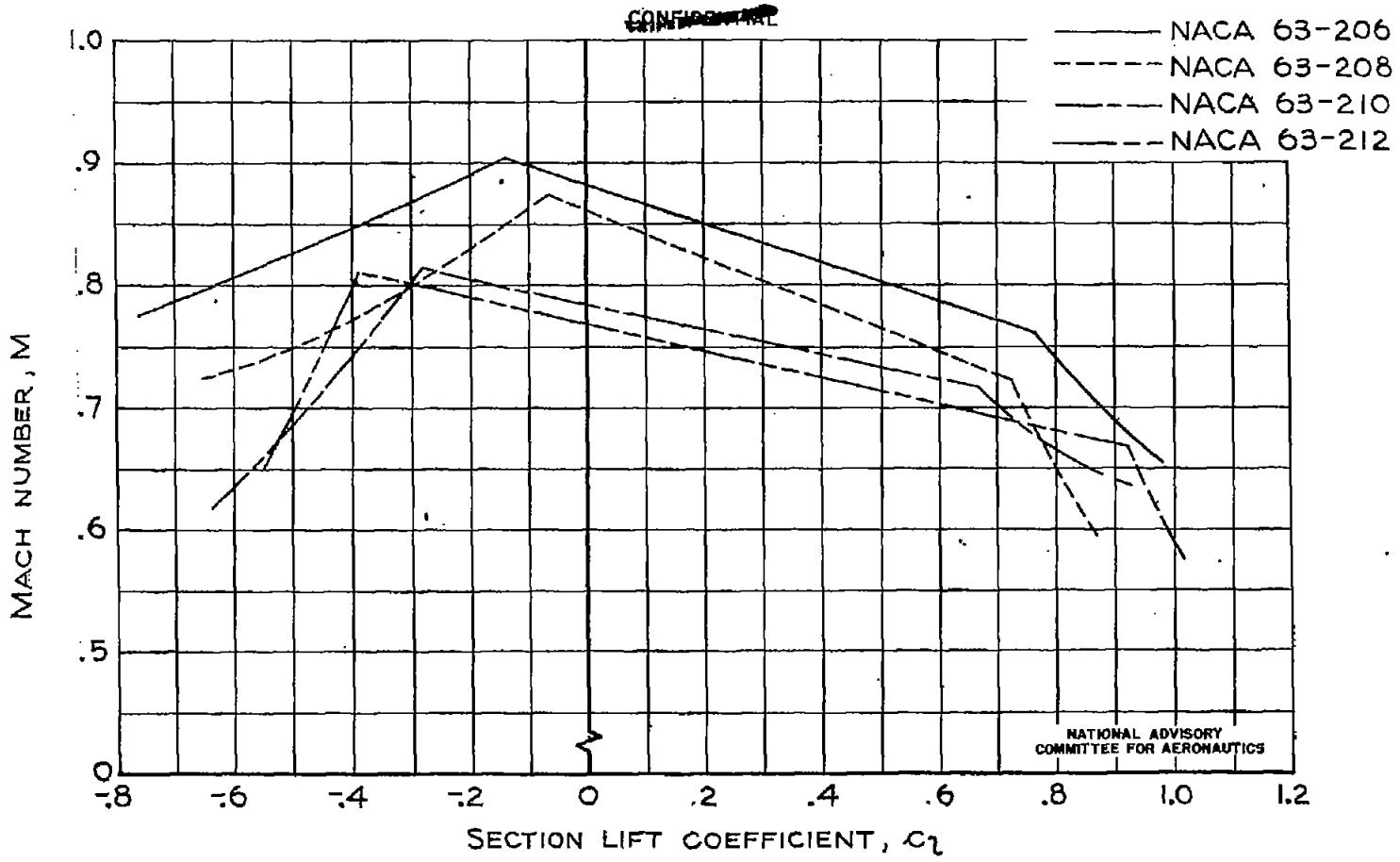

FIGURE 13.— COMPARISON OF LIFT-DIVERGENCE MACH NUMBERS FOR NACA 63-SERIES AIRFOILS.

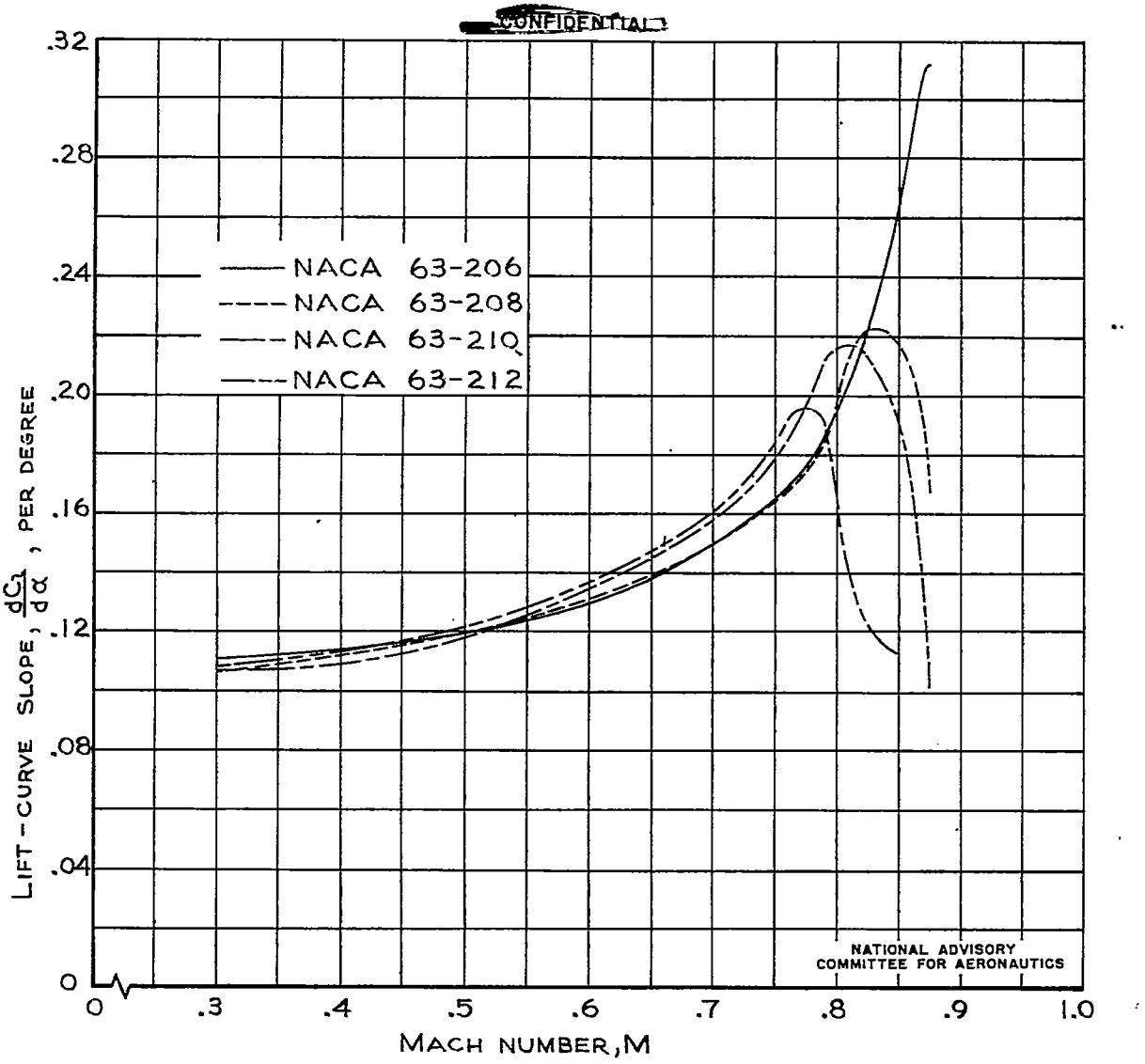

FIGURE 14.-THE VARIATION OF LIFT-CURVE SLOPE WITH MACH NUMBER AT THE DESIGN LIFT COEFFICIENT FOR NACA 63-SERIES AIRFOILS.

CONFIDENTIAL

CONFIDENTIAL

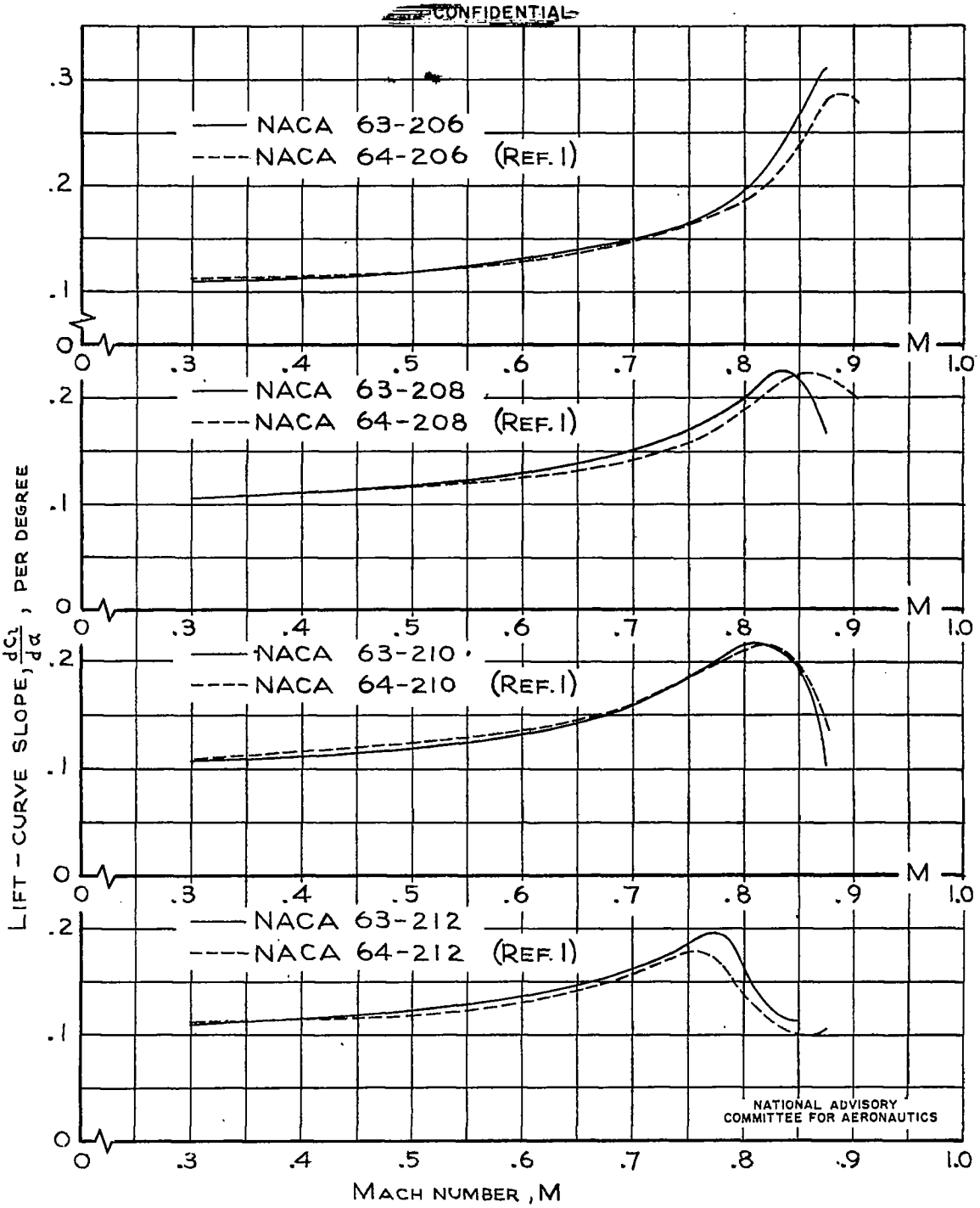

FIGURE 15.— COMPARISON OF THE VARIATION OF LIFT-CURVE SLOPE WITH MACH NUMBER AT THE DESIGN LIFT COEFFICIENT FOR NACA 63- AND 64-SERIES AIRFOILS.

CONFIDENTIAL

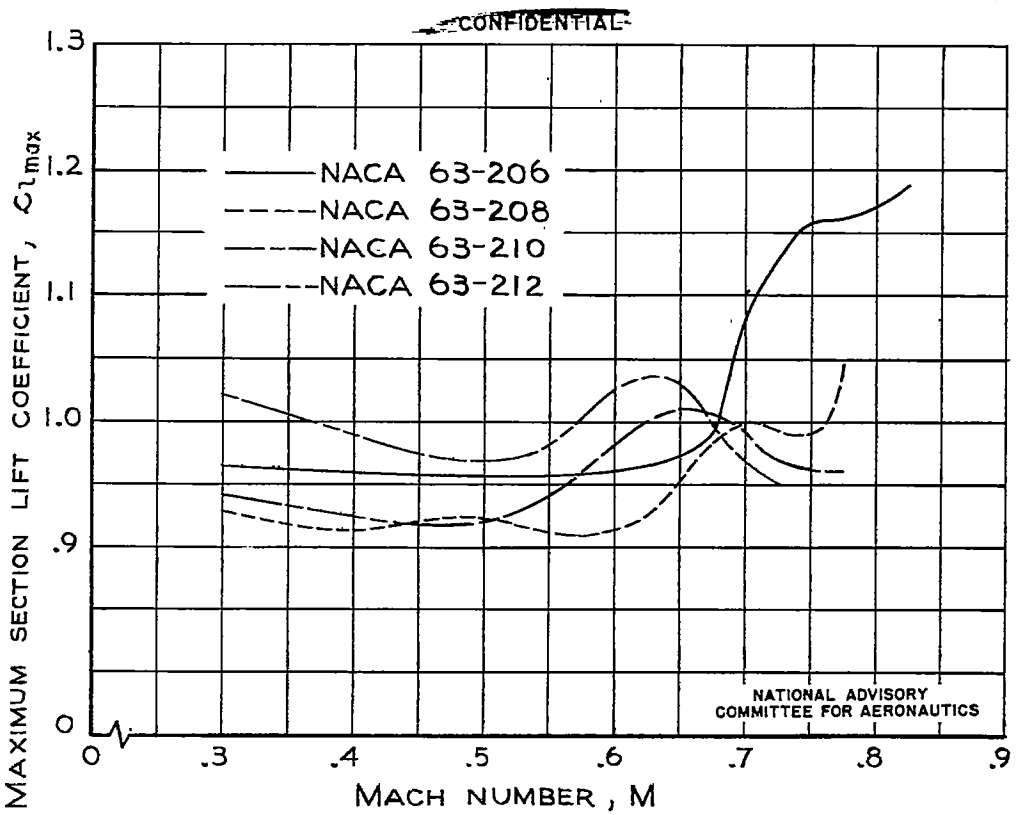

FIGURE 16.- THE VARIATION OF MAXIMUM SECTION LIFT COEFFICIENT WITH MACH NUMBER FOR NACA 63-SERIES AIRFOILS.

CONFIDENTIAL

CONFIDENTIAL

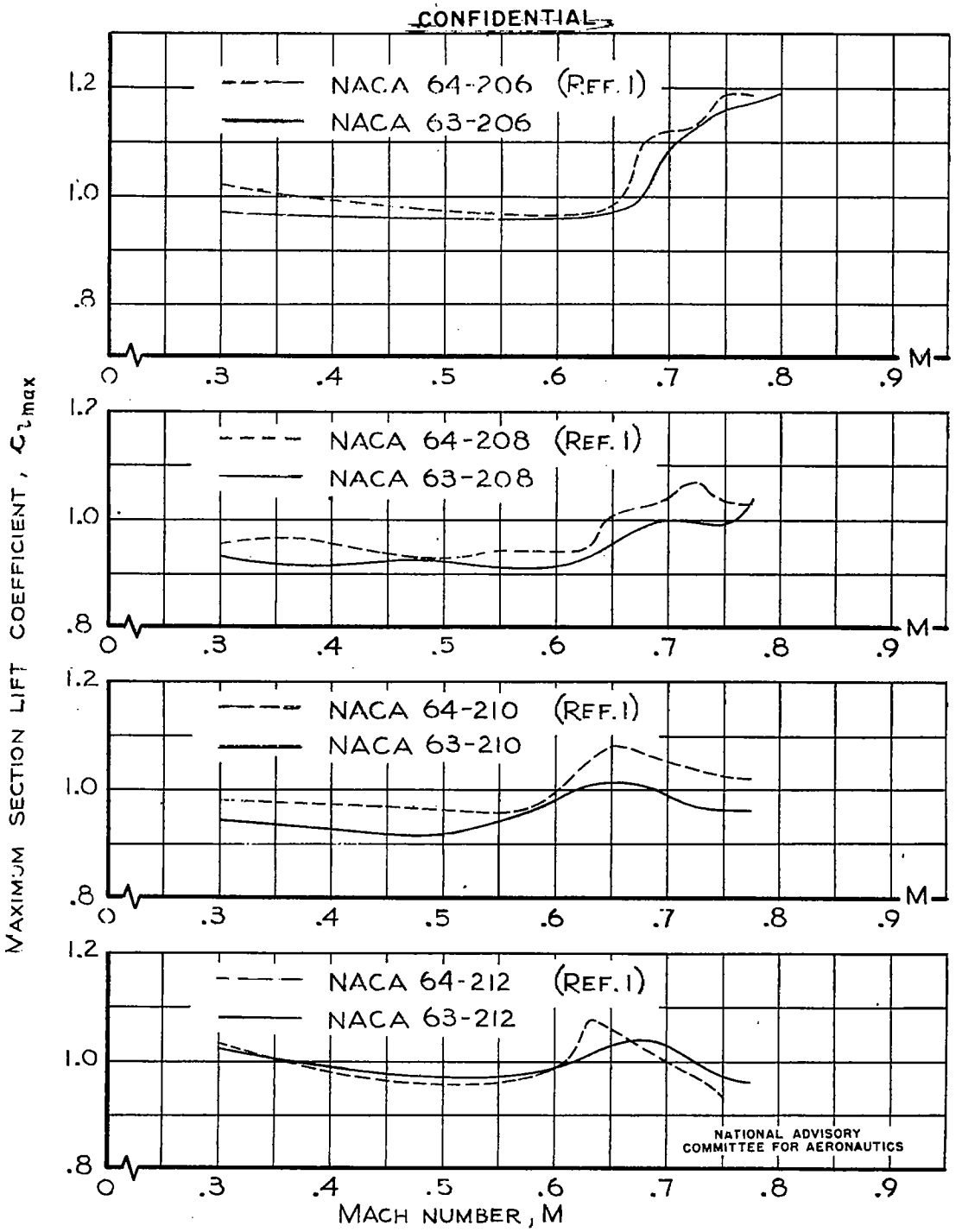

FIGURE 17.— COMPARISON OF THE VARIATION OF MAXIMUM SECTION LIFT COEFFICIENT WITH MACH NUMBER FOR NACA 63- AND 64-SERIES AIRFOILS.

CONFIDENTIAL

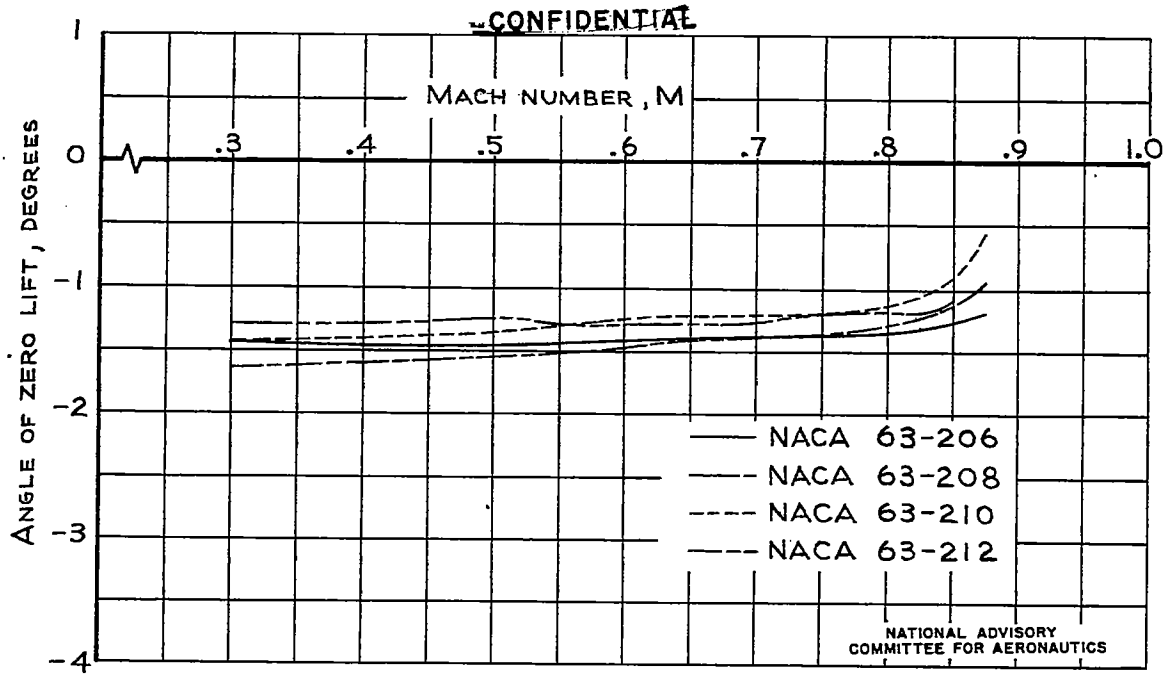

FIGURE 18.-THE VARIATION OF ANGLE OF ZERO LIFT WITH MACH NUMBER FOR NACA 63-SERIES AIRFOILS.

CONFIDENTIAL

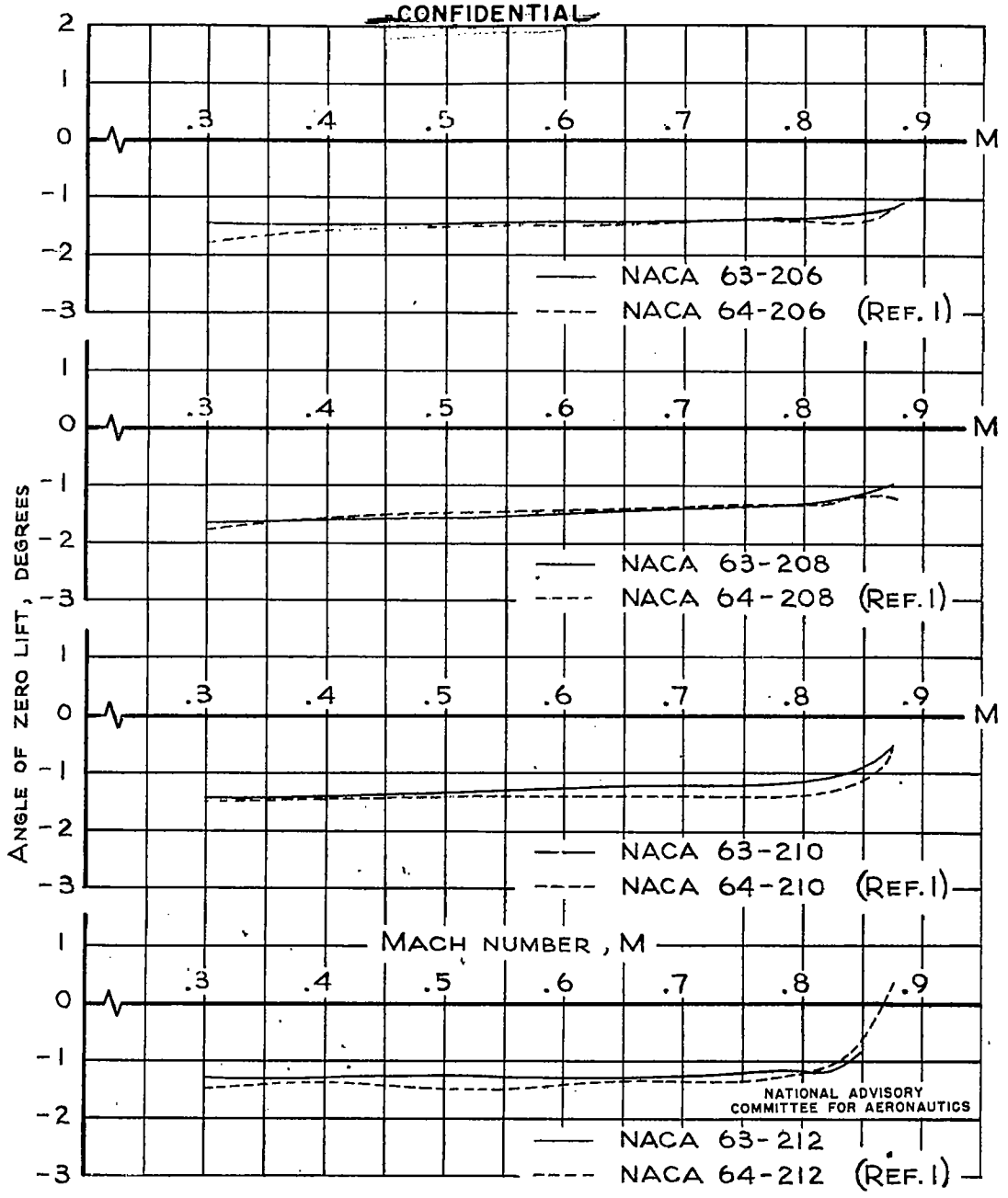

FIGURE 19.— COMPARISON OF THE VARIATION OF ANGLE OF ZERO LIFT WITH MACH NUMBER FOR NACA 63- AND 64- SERIES AIRFOILS.

CONFIDENTIAL

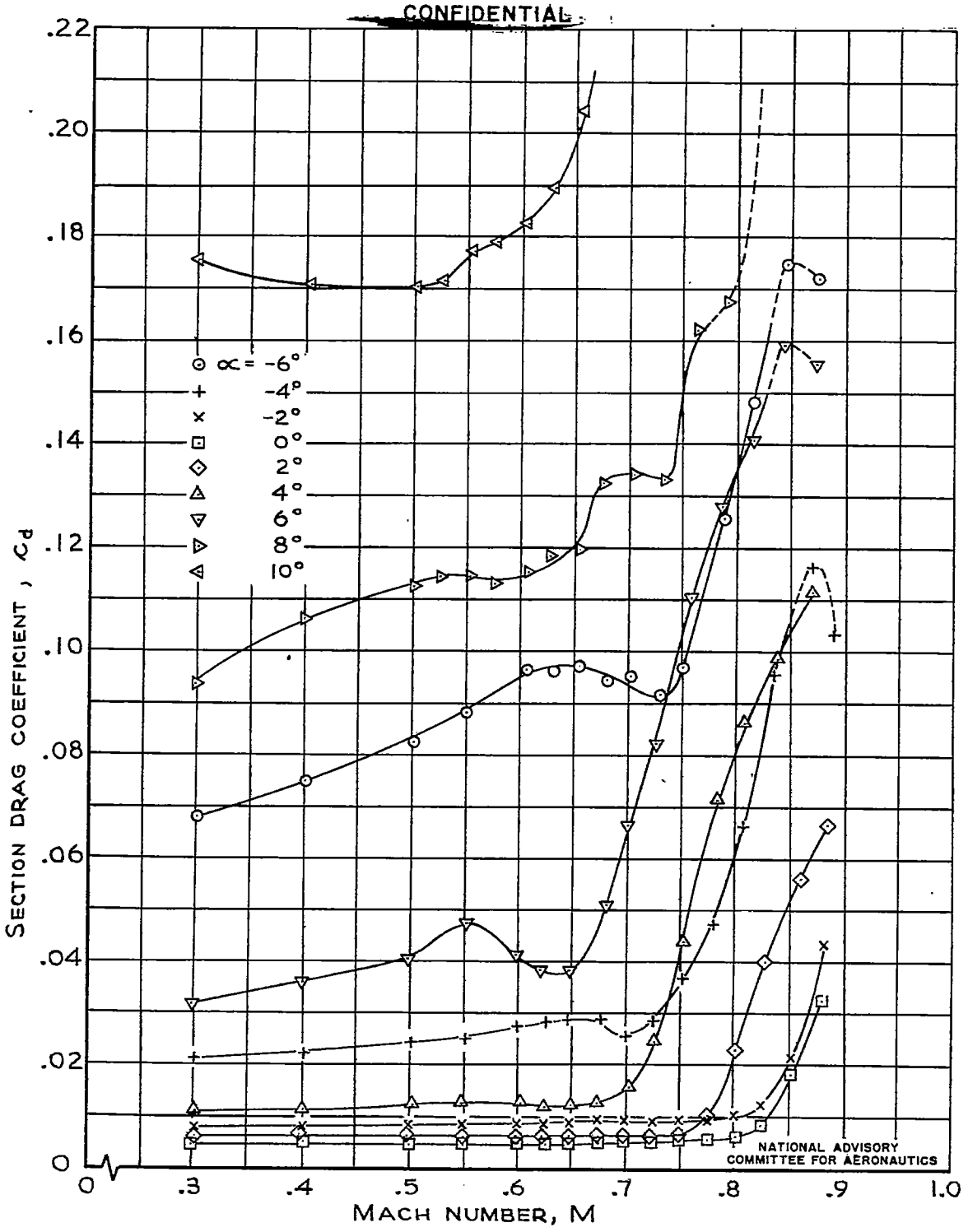

FIGURE 20.-THE VARIATION OF SECTION DRAG COEFFICIENT WITH MACH NUMBER FOR THE NACA 63-206 AIRFOIL.

CONFIDENTIAL

CONFIDENTIAL

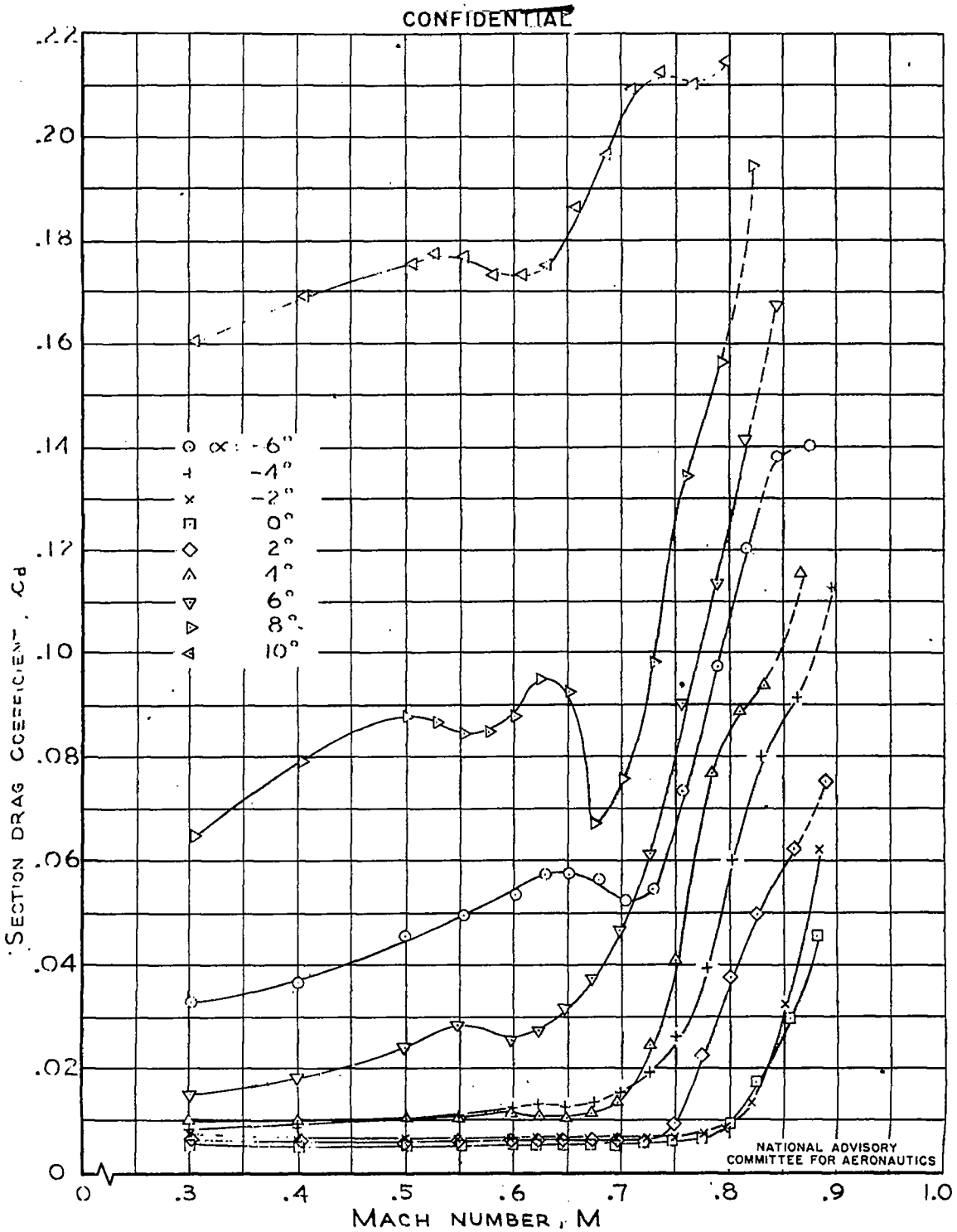

FIGURE 21.- THE VARIATION OF SECTION DRAG COEFFICIENT WITH MACH NUMBER FOR THE NACA 63-208 AIRFOIL.
CONFIDENTIAL

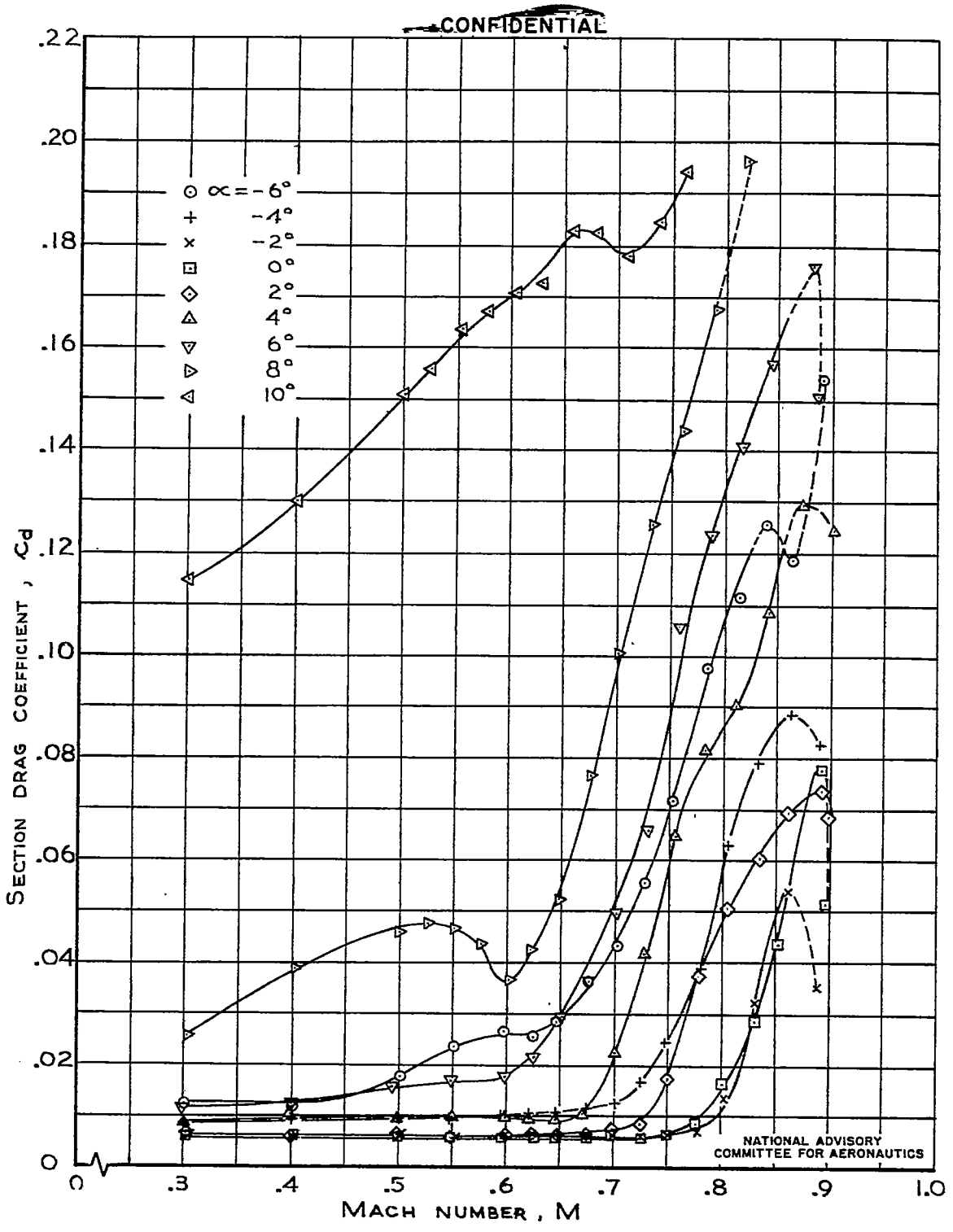

FIGURE 22.- THE VARIATION OF SECTION DRAG COEFFICIENT WITH MACH NUMBER FOR THE NACA 63-210 AIRFOIL.

CONFIDENTIAL

CONFIDENTIAL

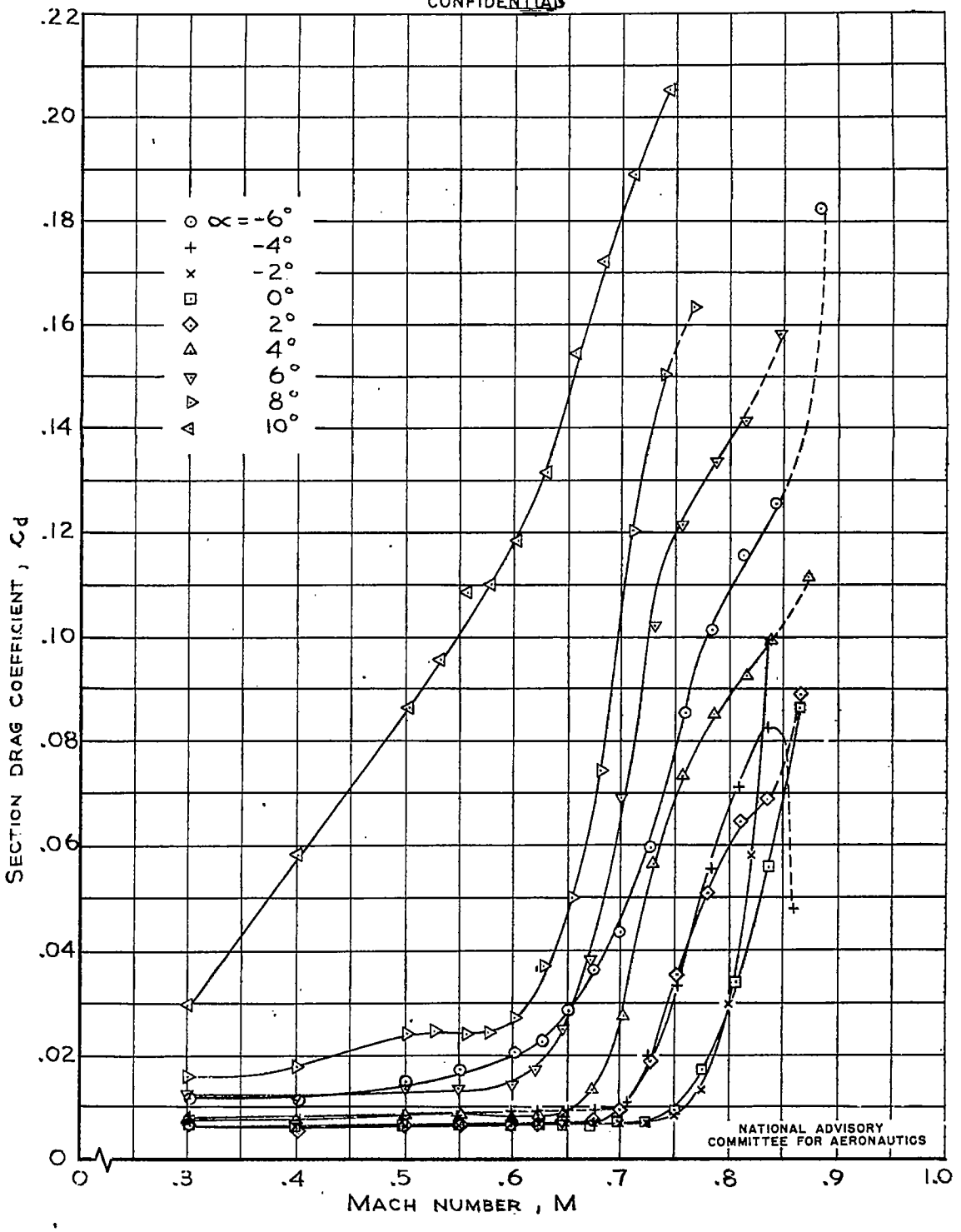

FIGURE 23.- THE VARIATION OF SECTION DRAG COEFFICIENT WITH MACH NUMBER FOR THE NACA 63-212 AIRFOIL.

CONFIDENTIAL

CONFIDENTIAL

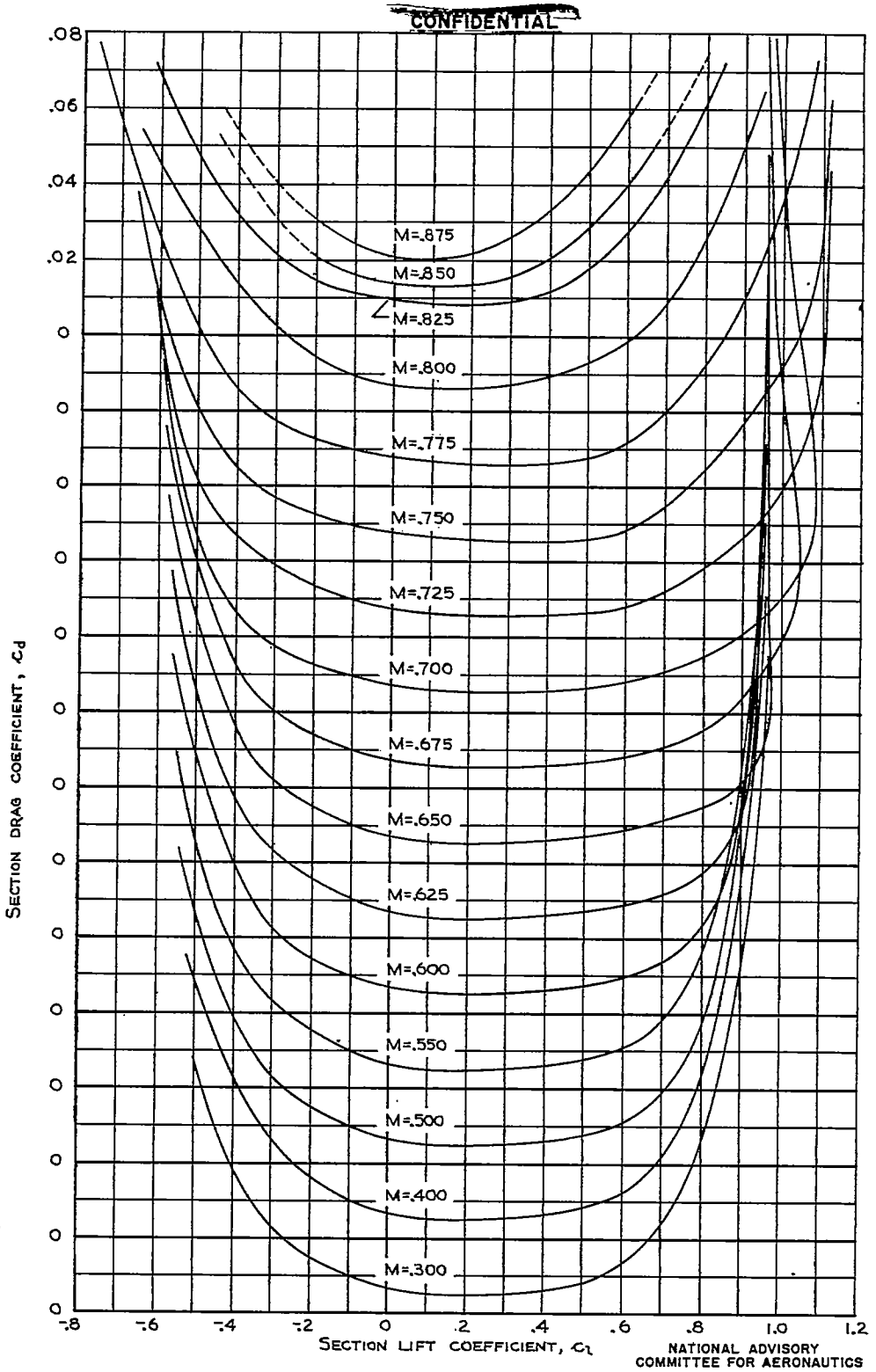

FIGURE 24.- THE VARIATION OF SECTION DRAG COEFFICIENT WITH LIFT COEFFICIENT FOR THE NACA 63-206 AIRFOIL.

CONFIDENTIAL

CONFIDENTIAL

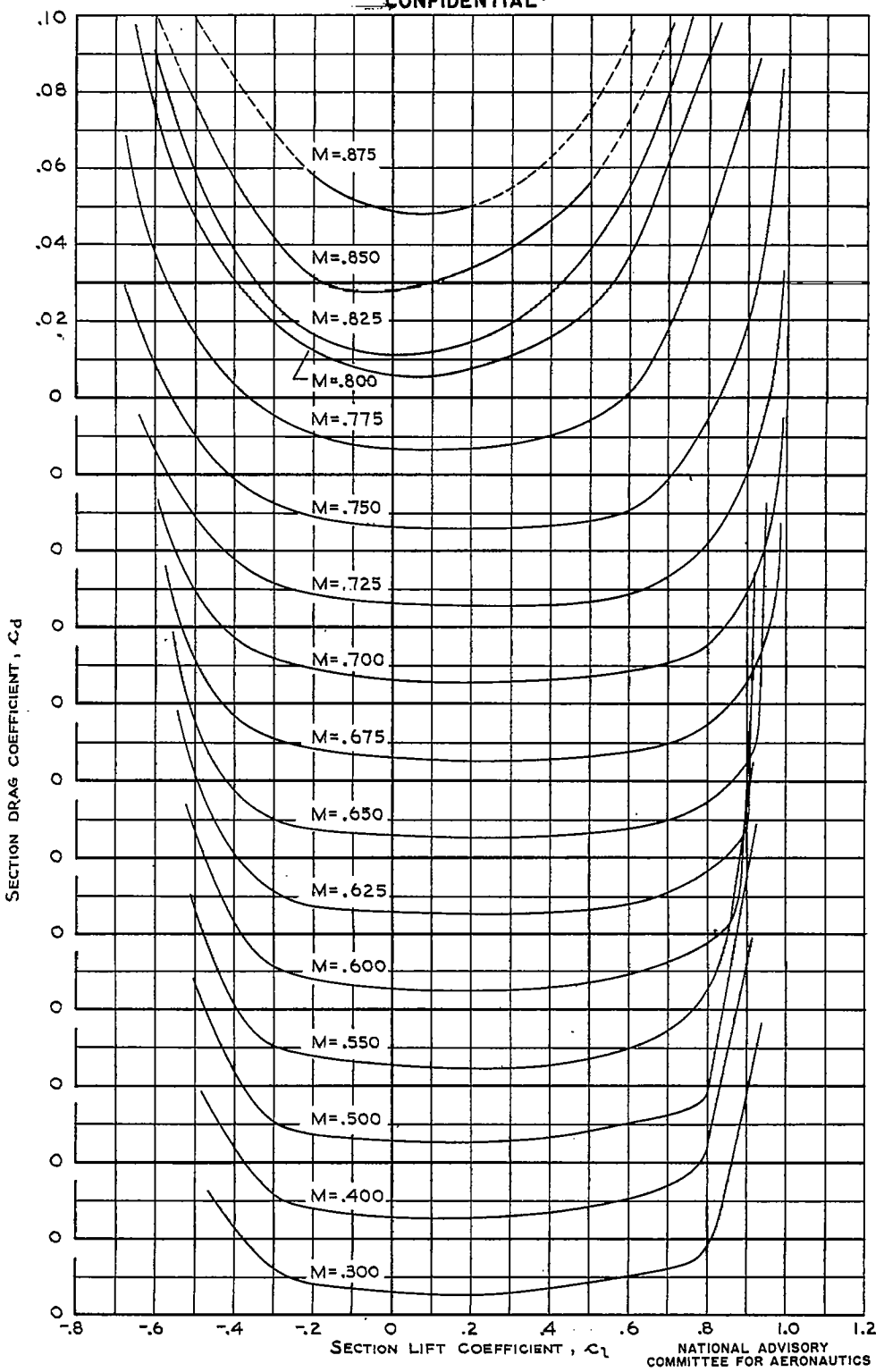

FIGURE 25.- THE VARIATION OF SECTION DRAG COEFFICIENT WITH LIFT COEFFICIENT FOR THE NACA 63-208 AIRFOIL.

CONFIDENTIAL

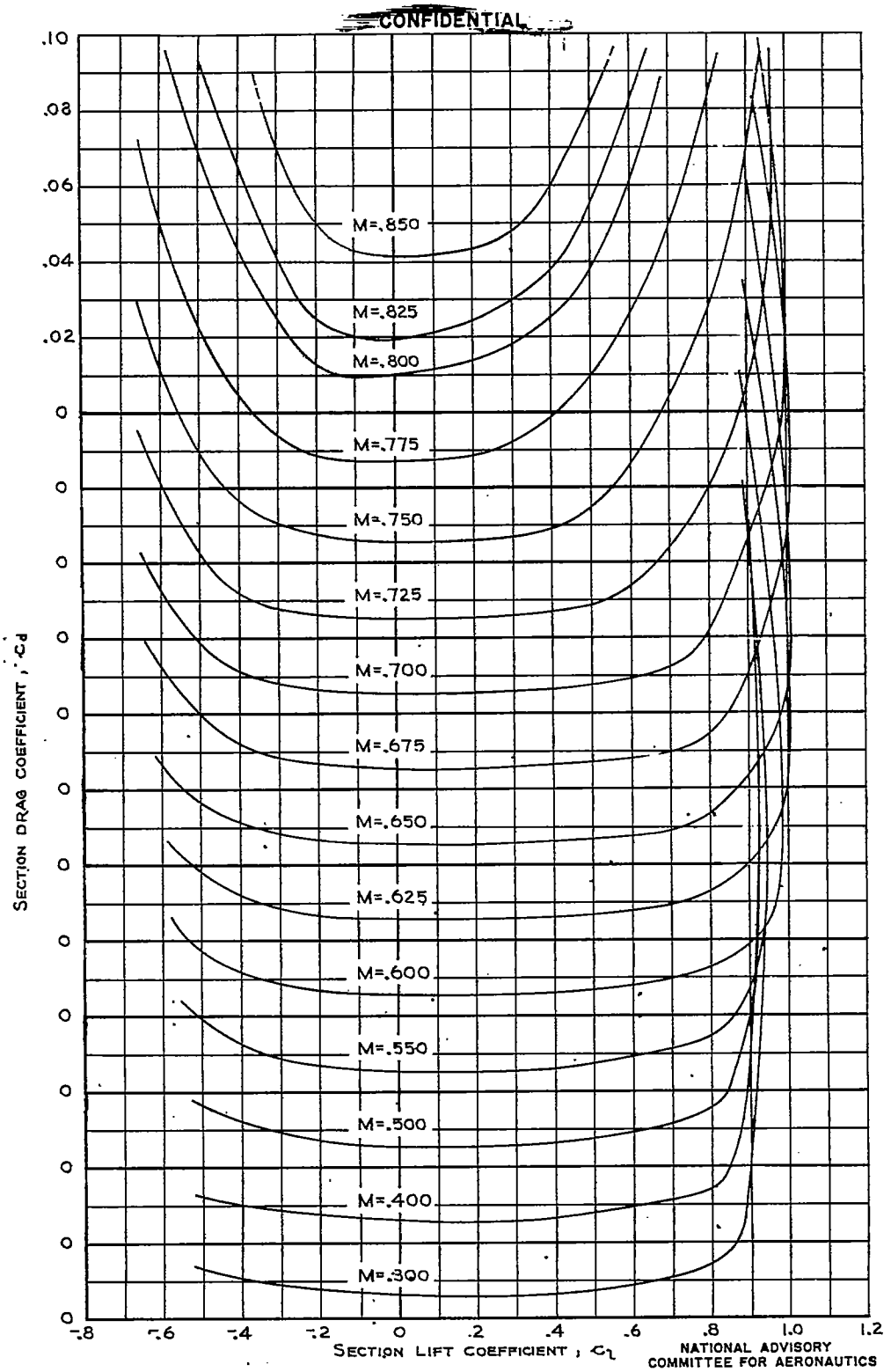

FIGURE 26.- THE VARIATION OF SECTION DRAG COEFFICIENT WITH LIFT COEFFICIENT FOR THE NACA 63-210 AIRFOIL.

CONFIDENTIAL

CONFIDENTIAL

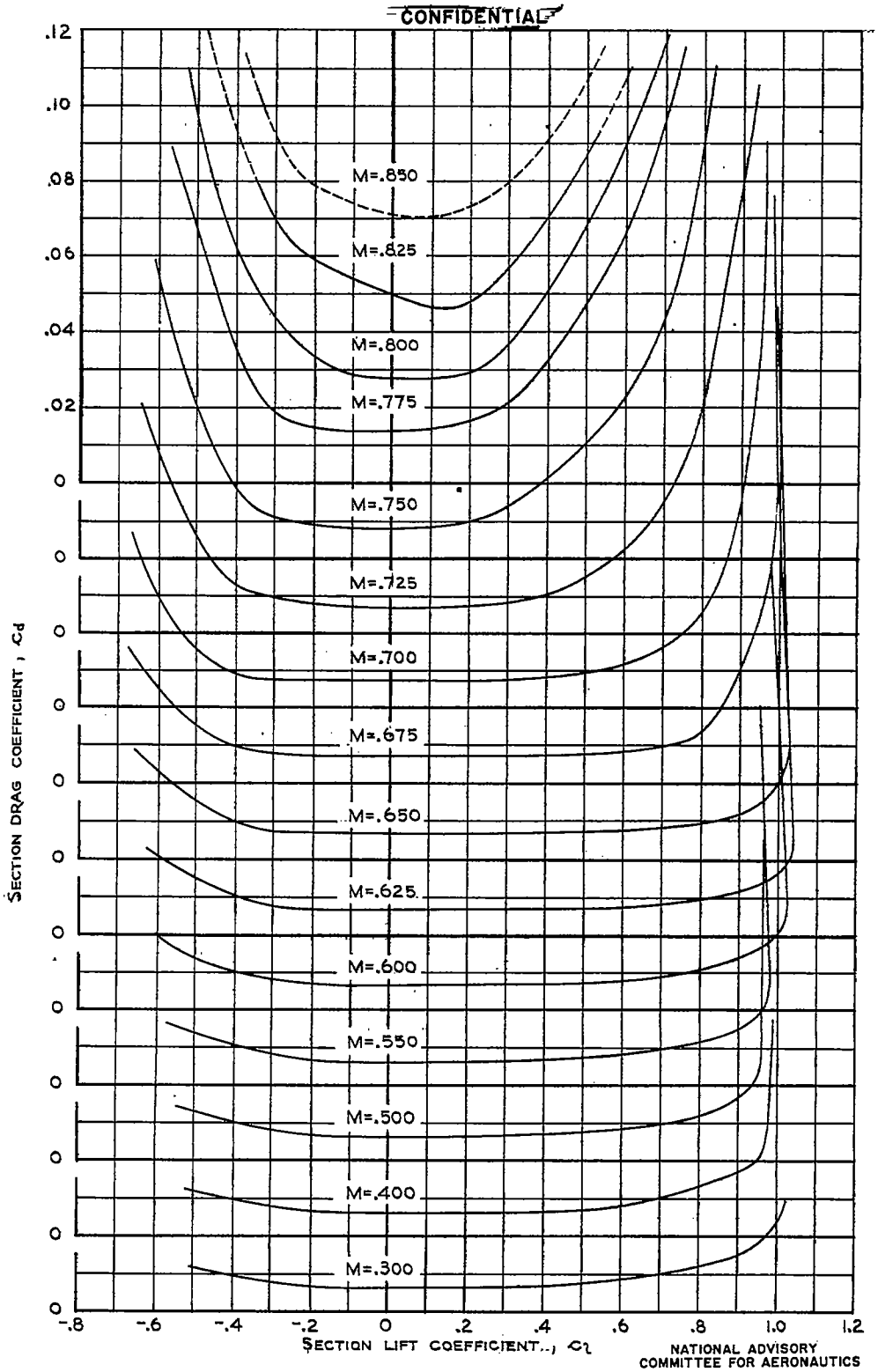

FIGURE 27.- THE VARIATION OF SECTION DRAG COEFFICIENT WITH LIFT COEFFICIENT FOR THE NACA 63-212 AIRFOIL.

CONFIDENTIAL

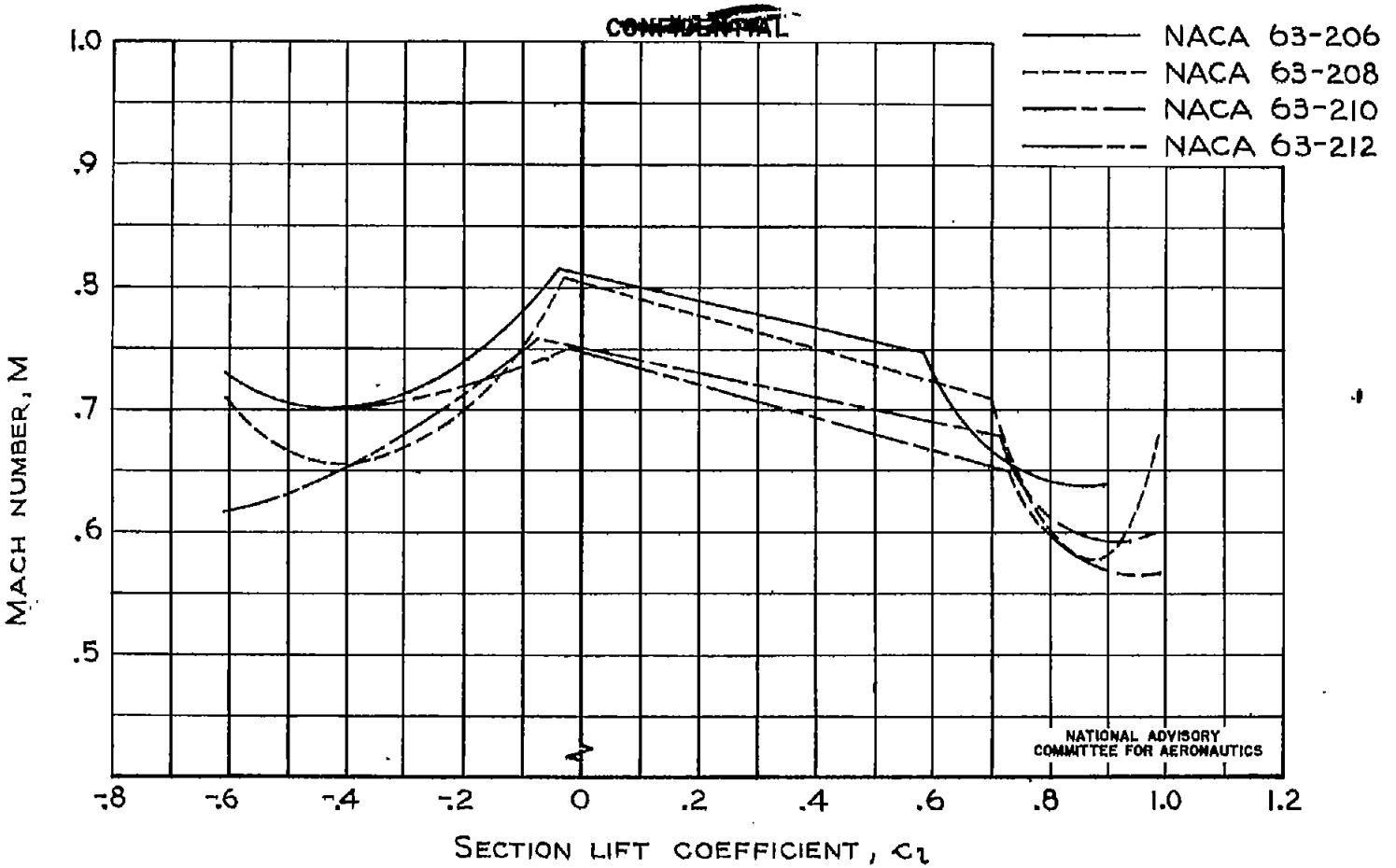

FIGURE 28.— COMPARISON OF DRAG-DIVERGENCE MACH NUMBERS FOR NACA 63-SERIES AIRFOILS.
CONFIDENTIAL

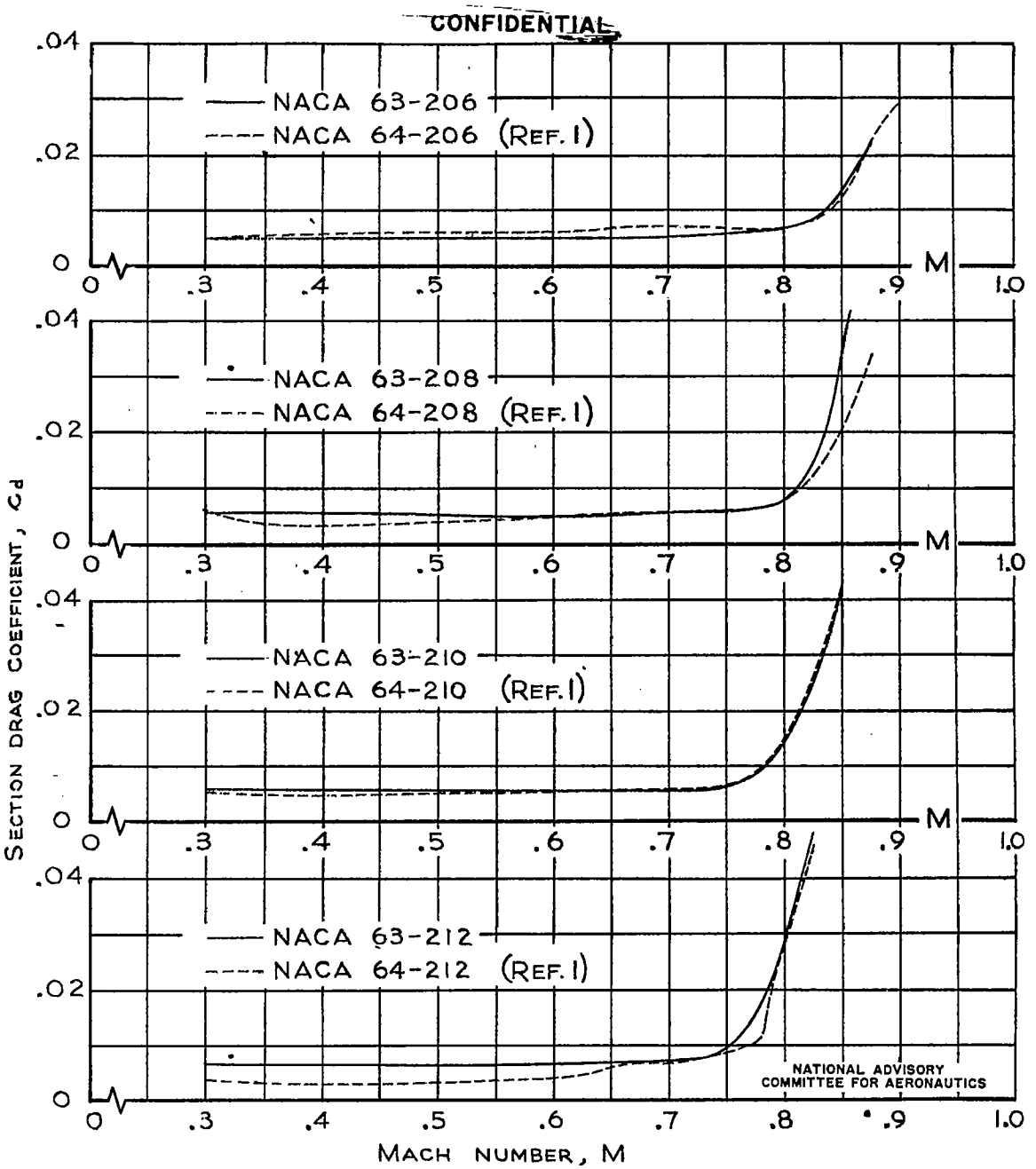

FIGURE 29.-THE VARIATION OF SECTION DRAG COEFFICIENT WITH MACH NUMBER AT THE DESIGN LIFT COEFFICIENT FOR NACA 63- AND 64-SERIES AIRFOIL SECTIONS.

CONFIDENTIAL

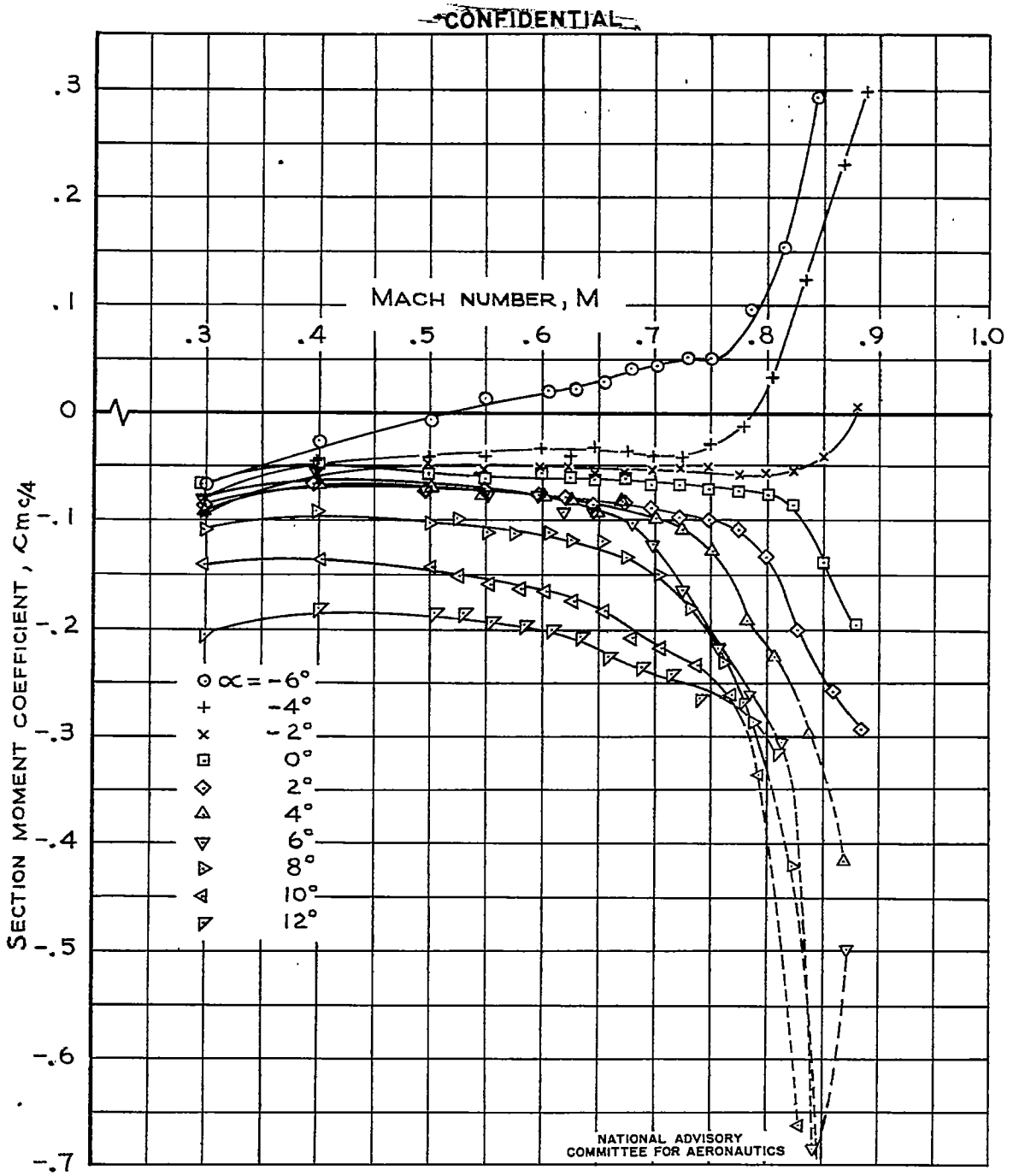

FIGURE 30.-THE VARIATION OF SECTION MOMENT COEFFICIENT WITH MACH NUMBER FOR THE NACA 63-206 AIRFOIL.

CONFIDENTIAL

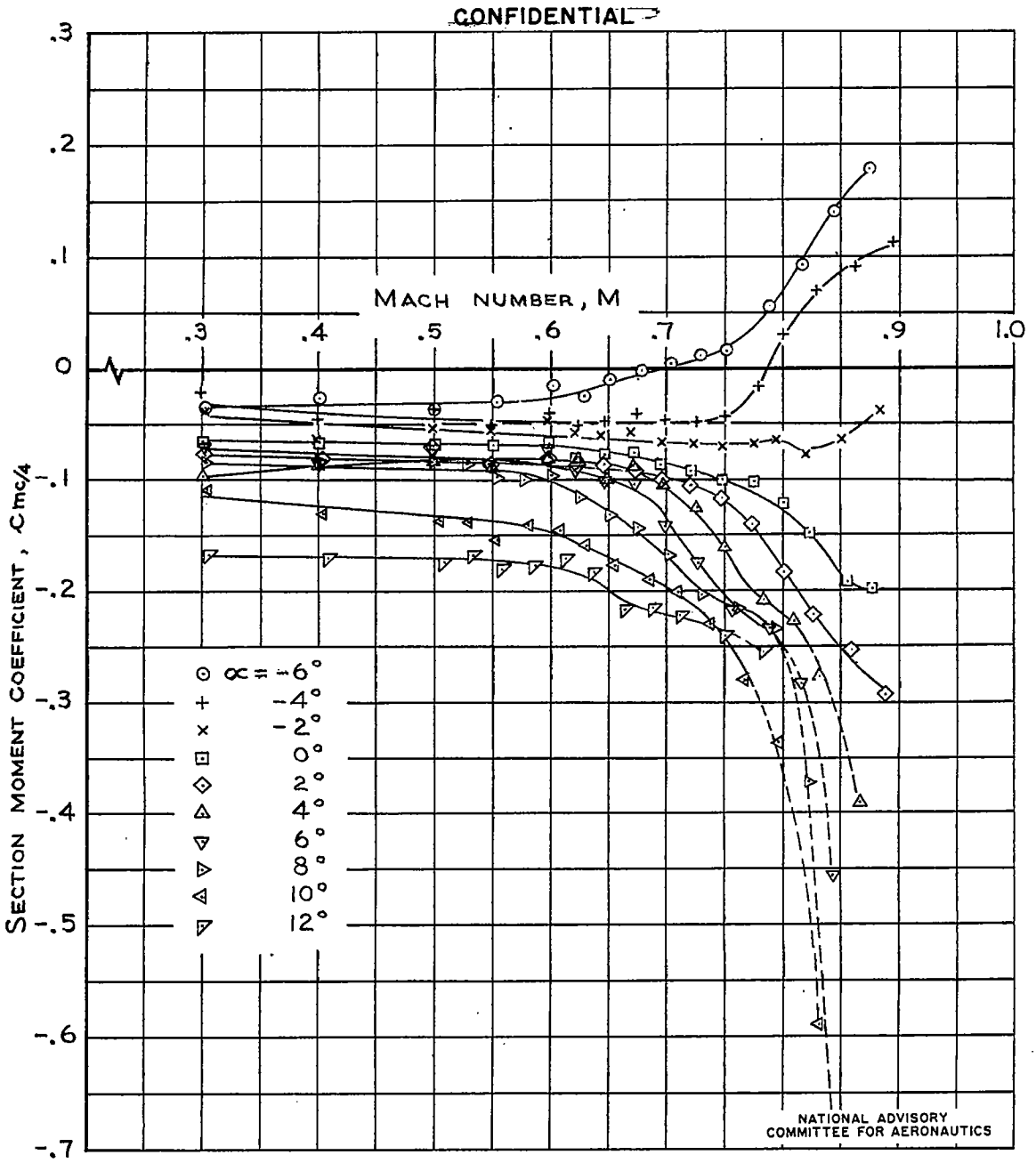

FIGURE 31.- THE VARIATION OF SECTION MOMENT COEFFICIENT WITH MACH NUMBER FOR THE NACA 63-208 AIRFOIL.

CONFIDENTIAL

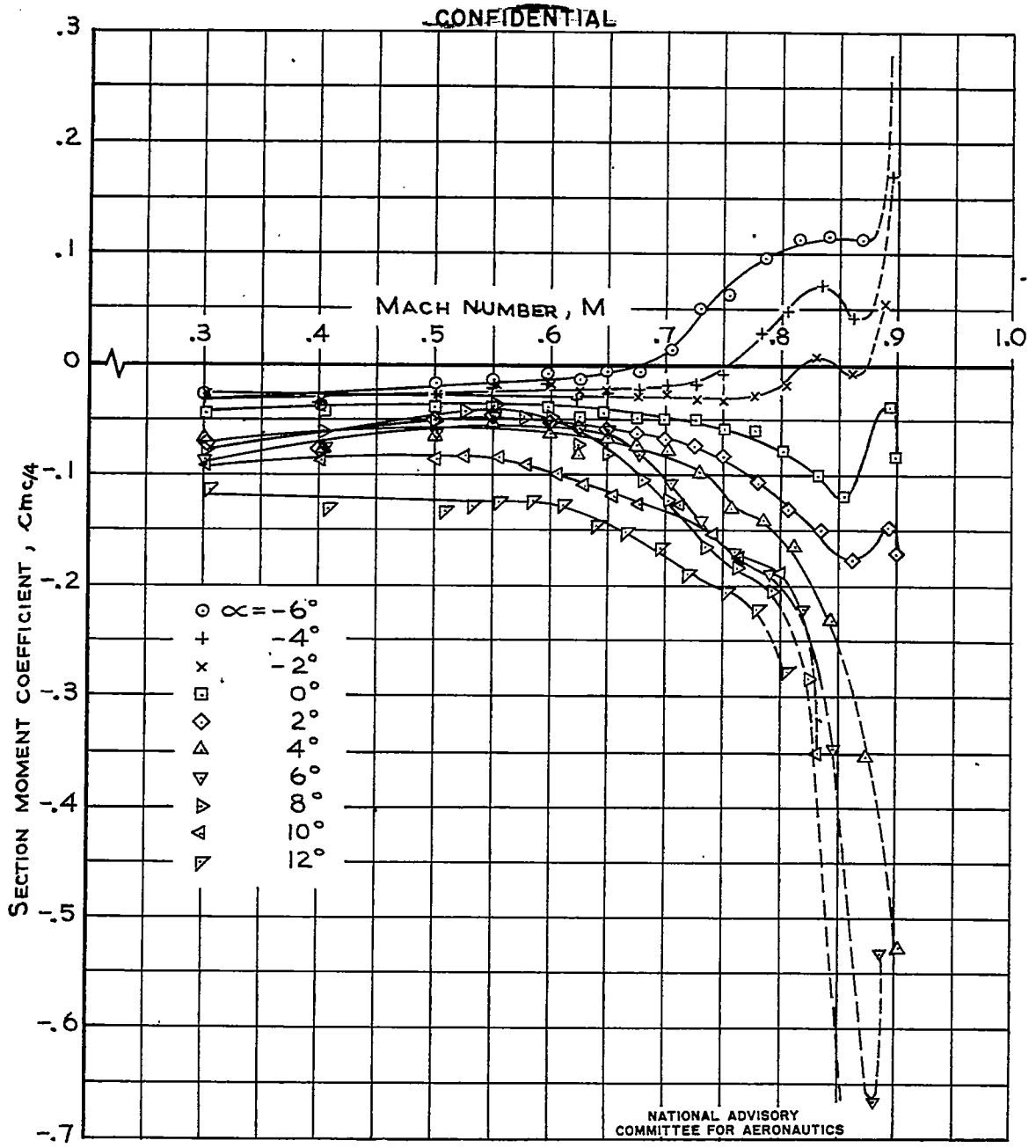

FIGURE 32.- THE VARIATION OF SECTION MOMENT COEFFICIENT WITH MACH NUMBER FOR THE NACA 63-210 AIRFOIL.

CONFIDENTIAL

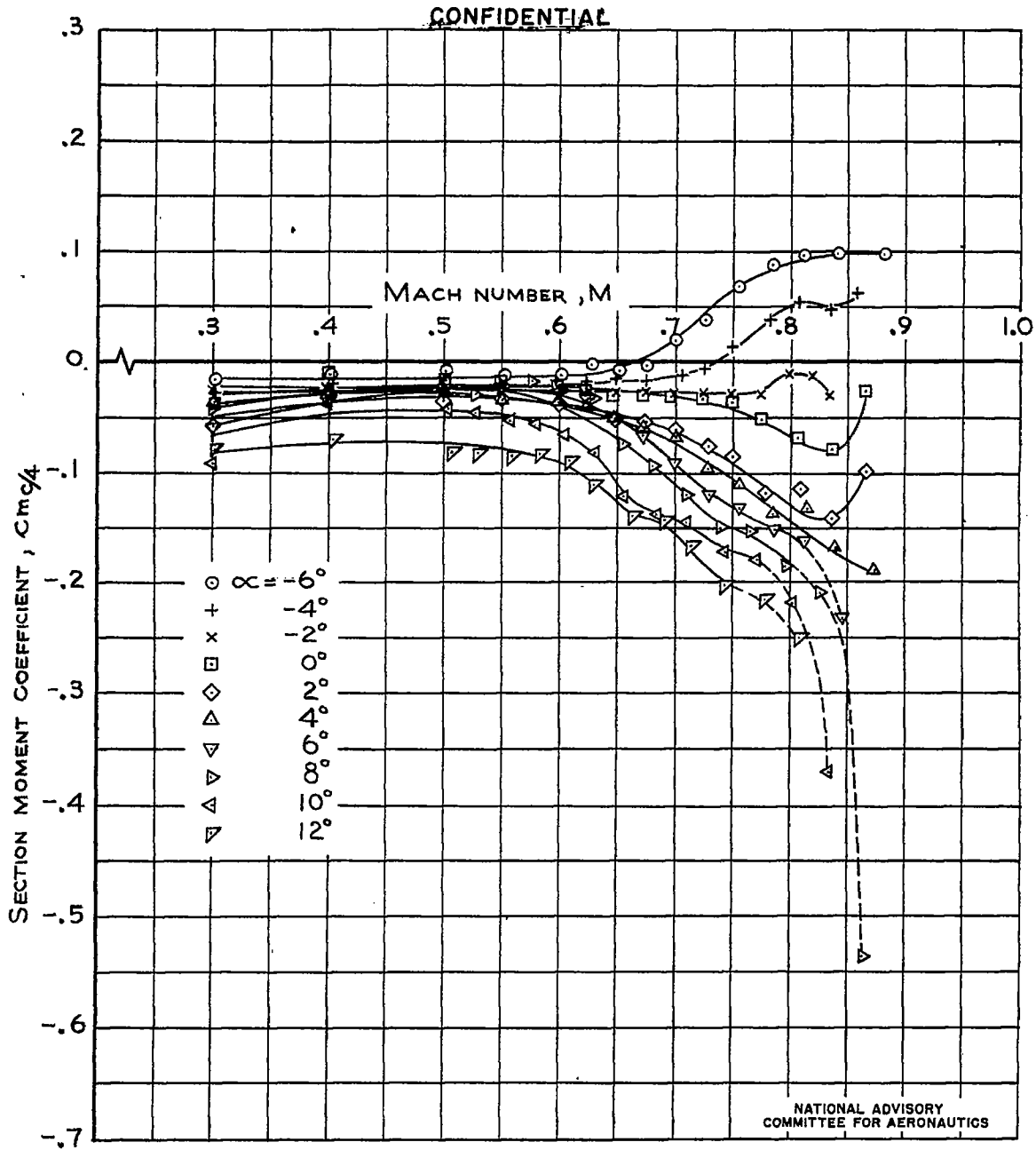

FIGURE 33.- THE VARIATION OF SECTION MOMENT COEFFICIENT WITH MACH NUMBER FOR THE NACA 63-212 AIRFOIL.
CONFIDENTIAL

CONFIDENTIAL

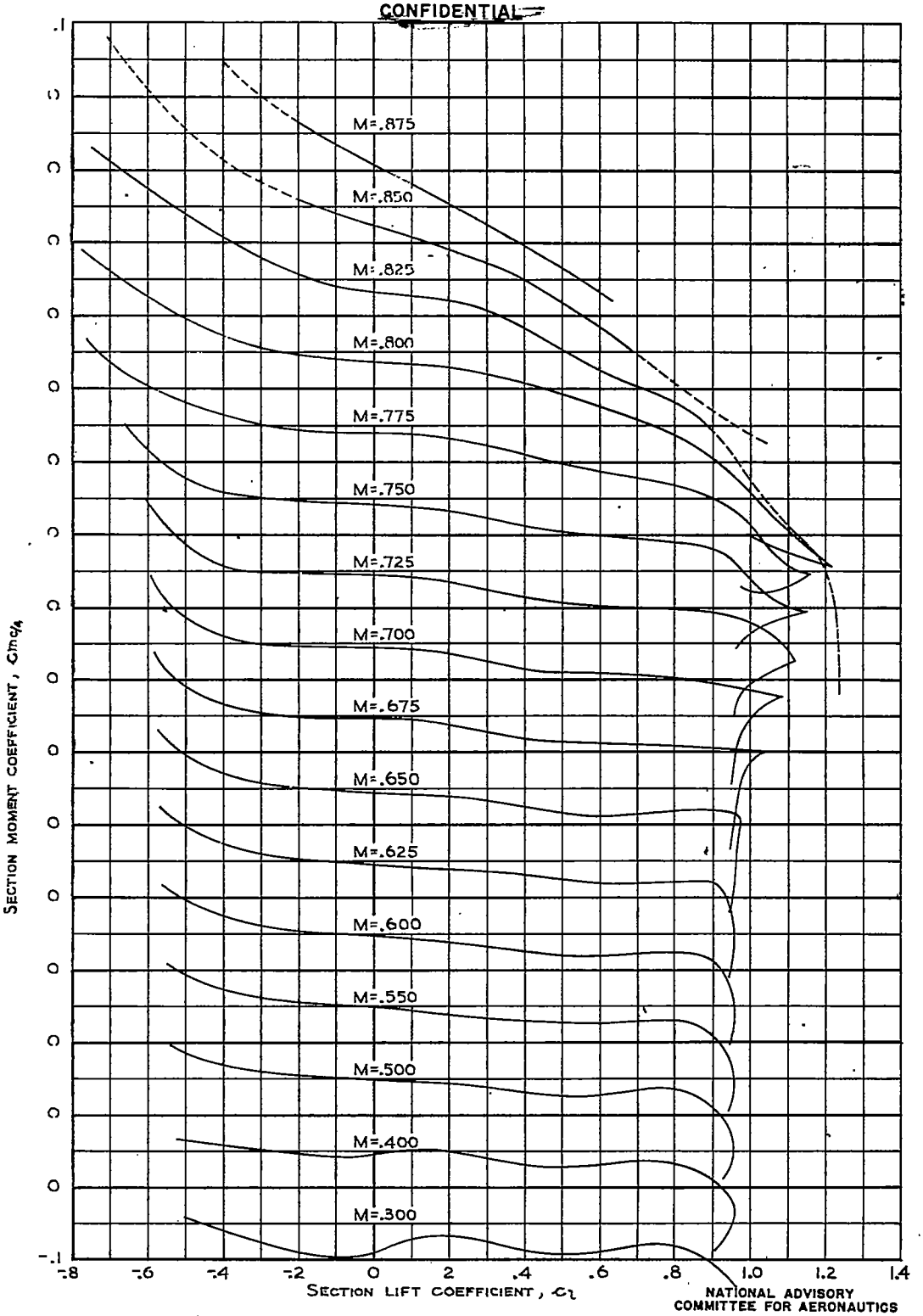

FIGURE 34.- THE VARIATION OF SECTION MOMENT COEFFICIENT WITH LIFT COEFFICIENT FOR THE NACA 63-206 AIRFOIL.

CONFIDENTIAL

CONFIDENTIAL

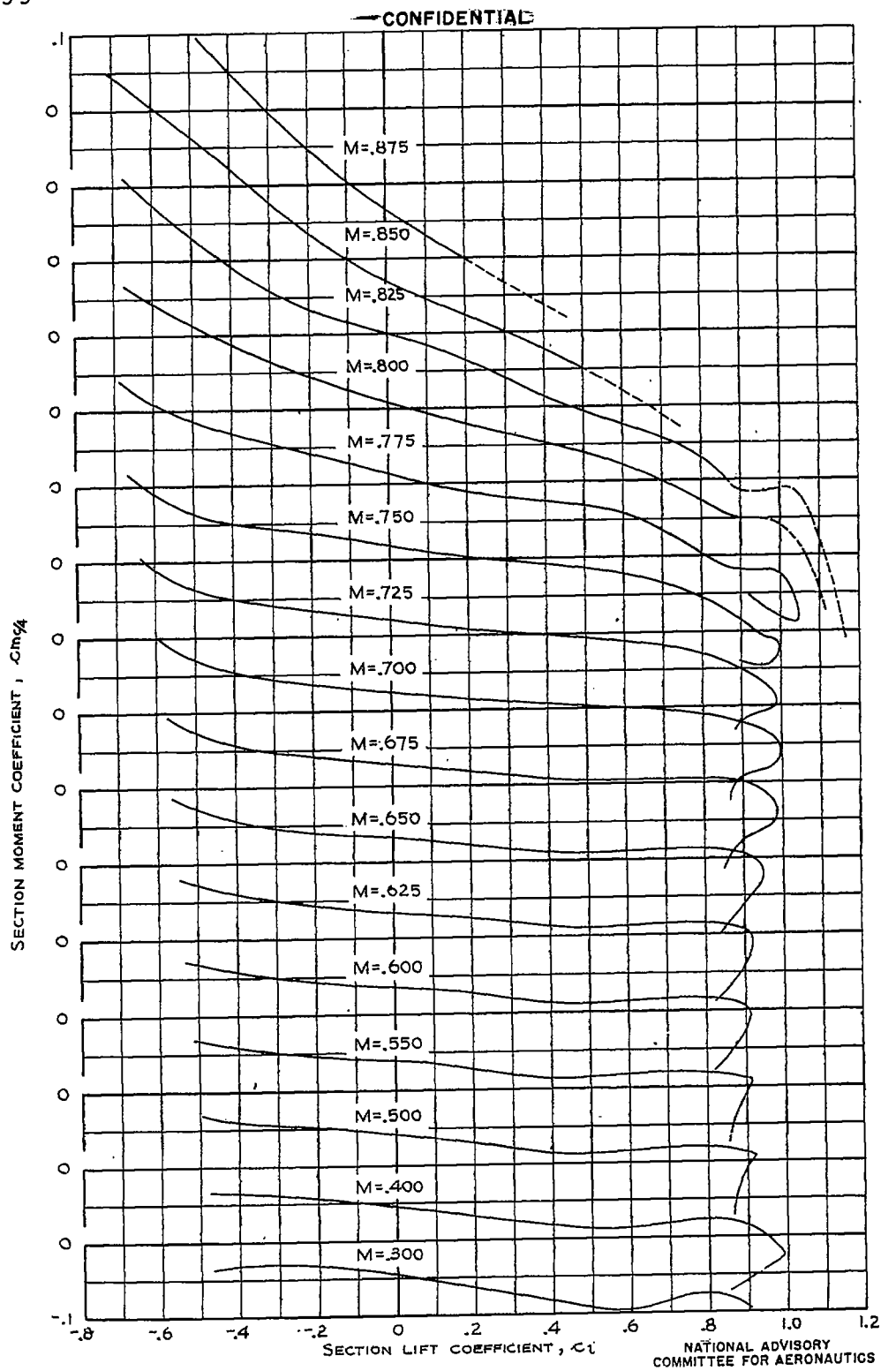

FIGURE 35.- THE VARIATION OF SECTION MOMENT COEFFICIENT WITH LIFT COEFFICIENT FOR THE NACA 63-208 AIRFOIL.

CONFIDENTIAL

CONFIDENTIAL

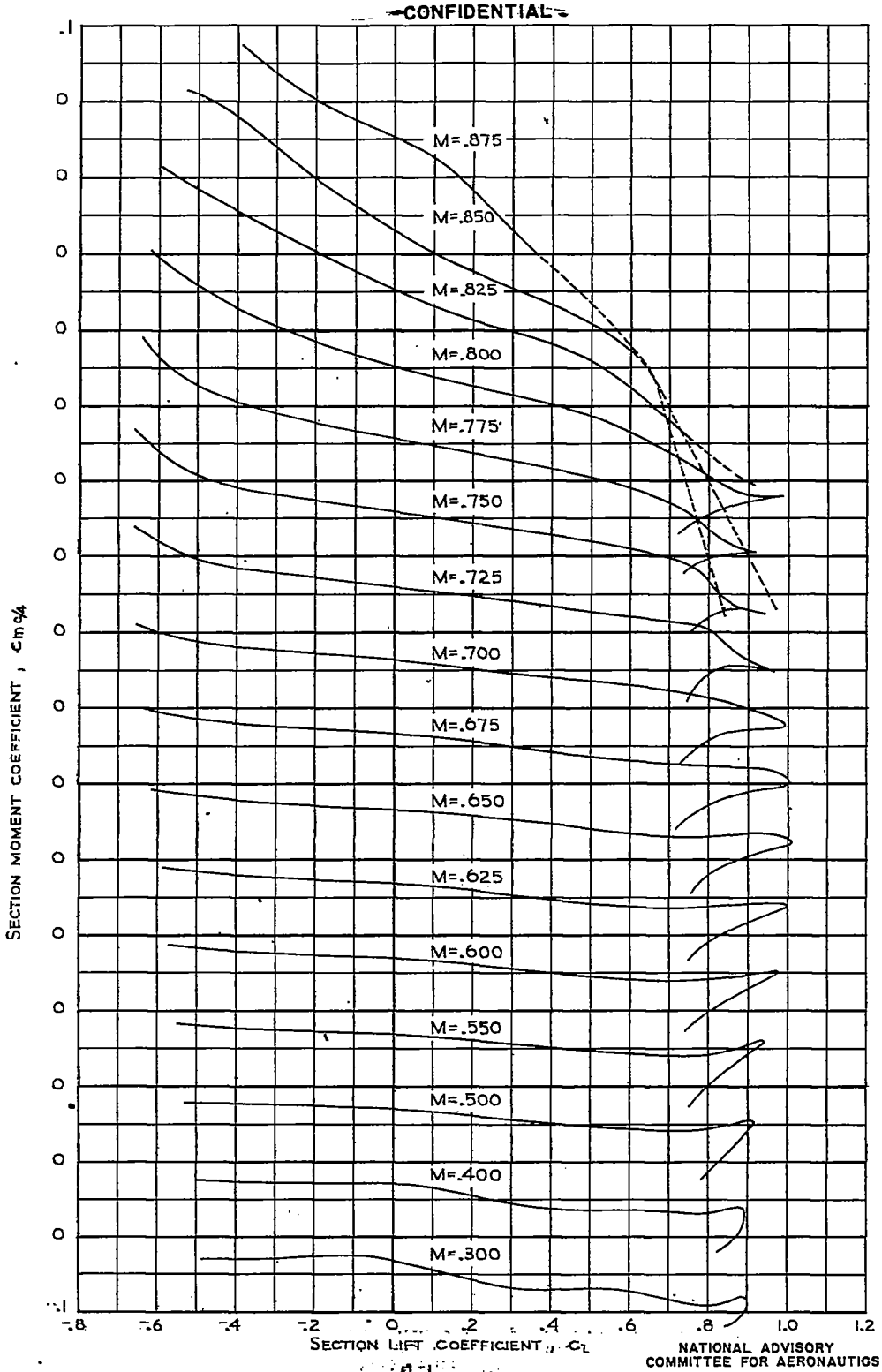

FIGURE 36.- THE VARIATION OF SECTION MOMENT COEFFICIENT WITH LIFT COEFFICIENT FOR THE NACA 63-210 AIRFOIL.

CONFIDENTIAL

CONFIDENTIAL

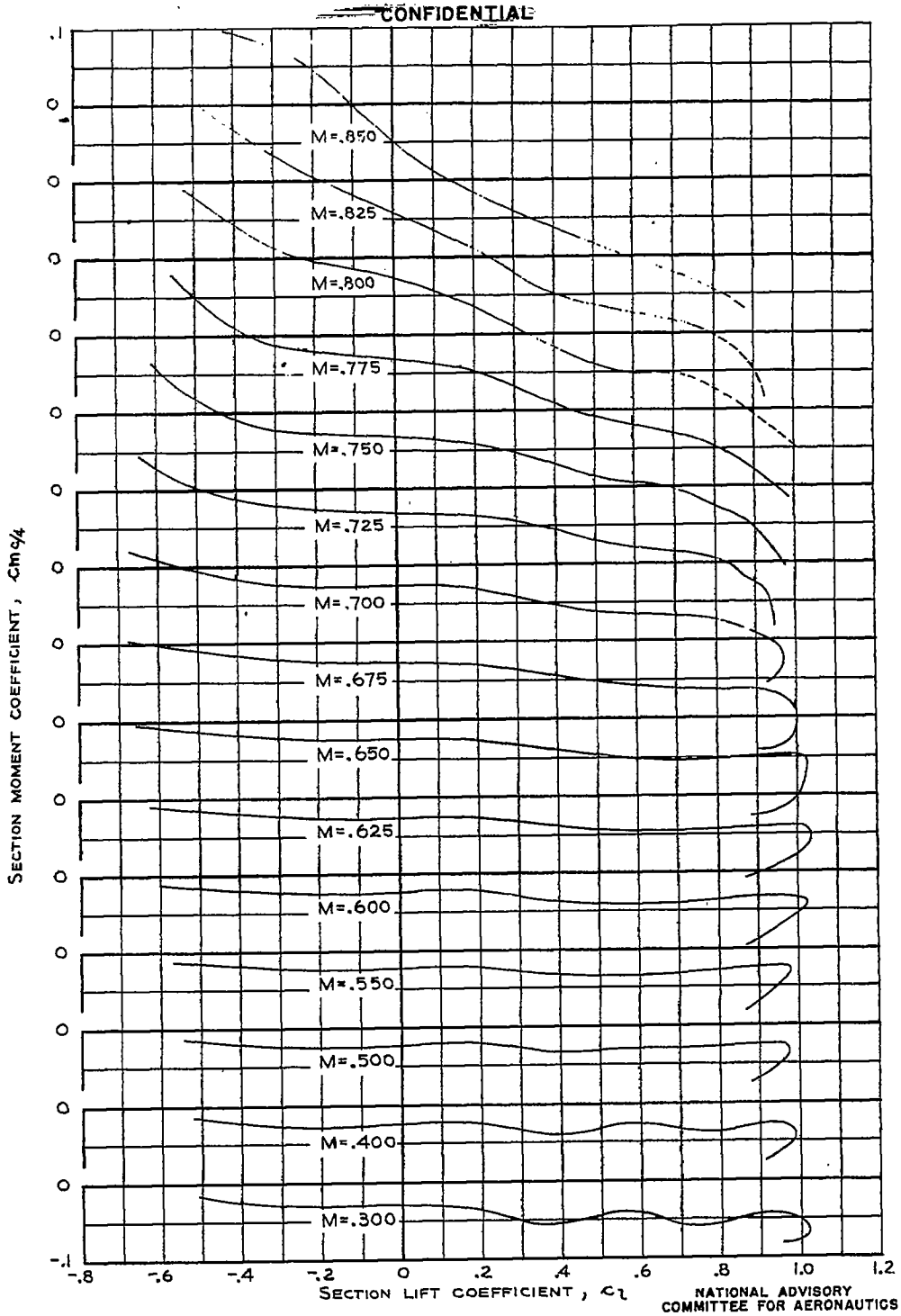

FIGURE 37.- THE VARIATION OF SECTION MOMENT COEFFICIENT WITH LIFT COEFFICIENT FOR THE NACA 63-212 AIRFOIL.

CONFIDENTIAL

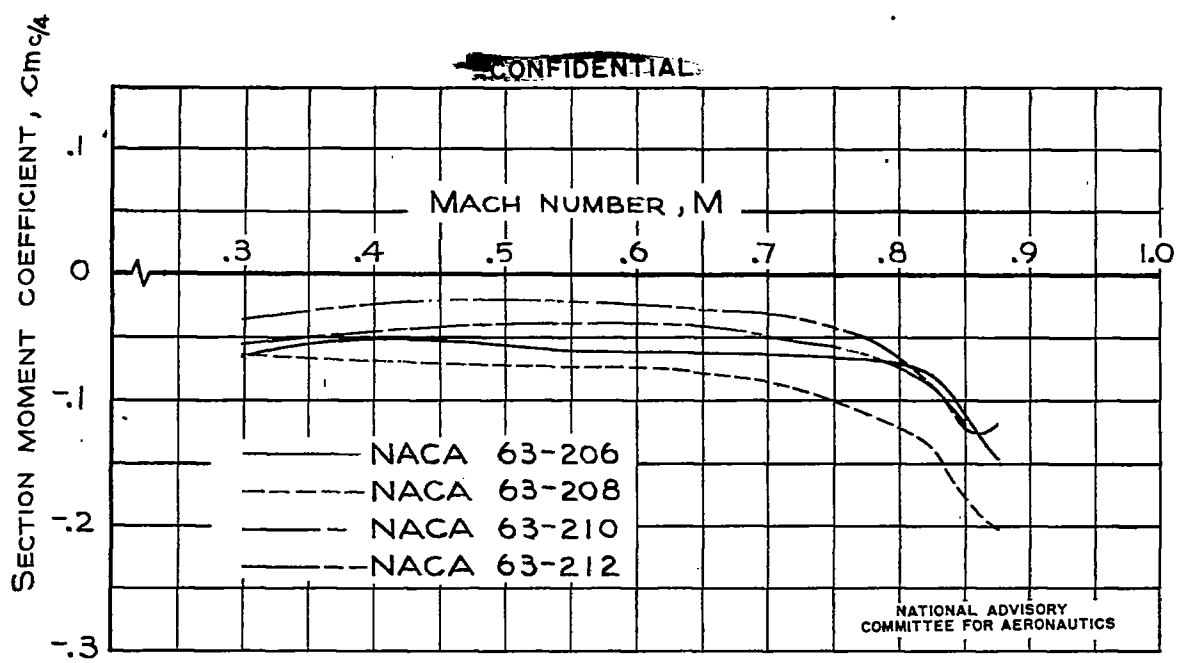

FIGURE 38.- THE VARIATION OF SECTION MOMENT COEFFICIENT WITH MACH NUMBER AT THE DESIGN LIFT COEFFICIENT FOR NACA 63-SERIES AIRFOILS.
CONFIDENTIAL

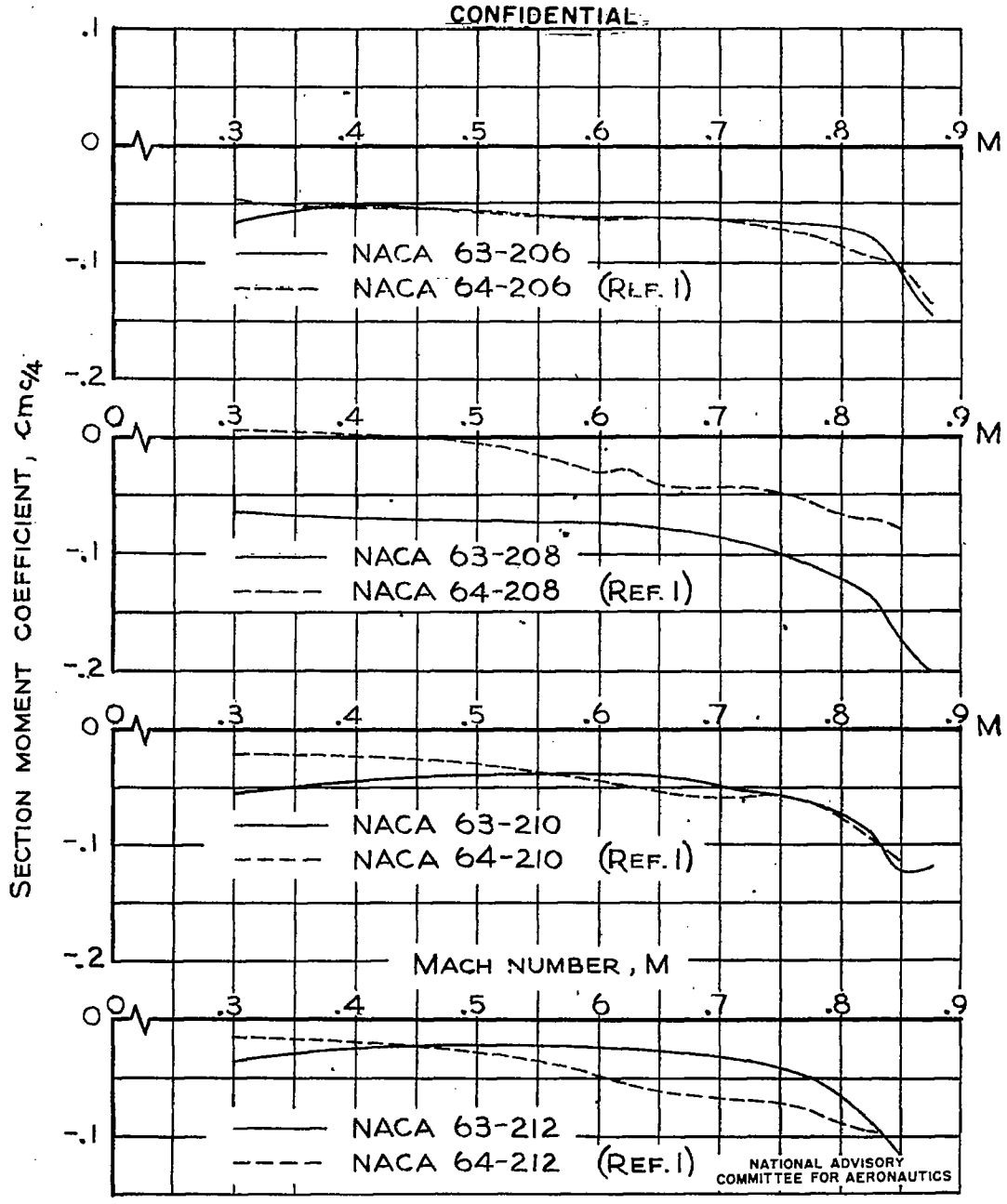

FIGURE 39.— COMPARISON OF THE VARIATION OF SECTION MOMENT COEFFICIENT WITH MACH NUMBER AT THE DESIGN LIFT COEFFICIENT FOR NACA 63- AND 64-SERIES AIRFOILS.

CONFIDENTIAL